Attosecond spectroscopy to track and control electron dynamics in matter

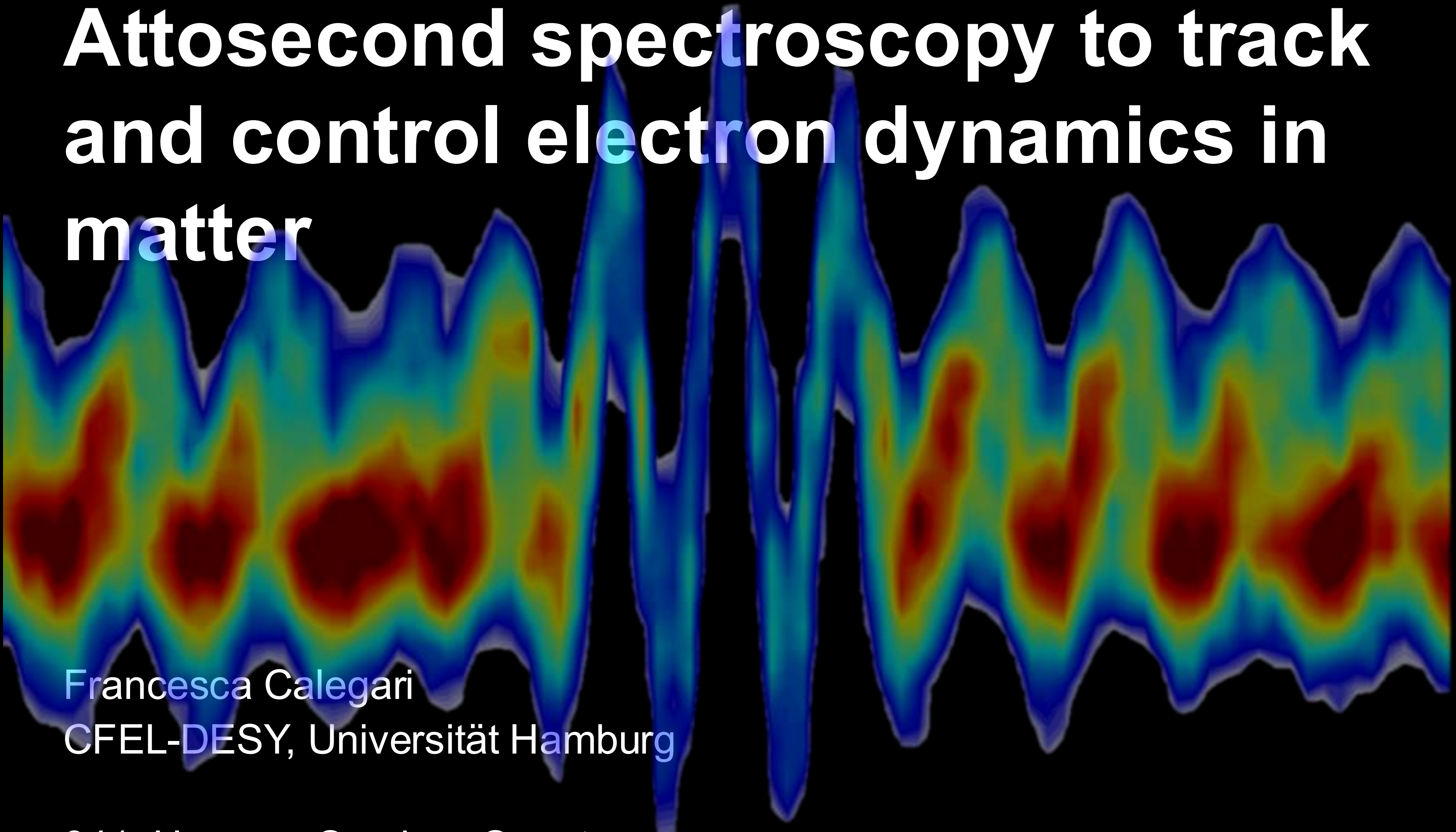

Francesca Calegari
CFEL-DESY, Universität Hamburg

841. Heraeus Seminar Quantum Technologies

CLUSTER OF EXCELLENCE
CUI: ADVANCED IMAGING OF MATTER

UHH

DESY.

Time scales in matter

Matter is often driven by external stimuli out of equilibrium!

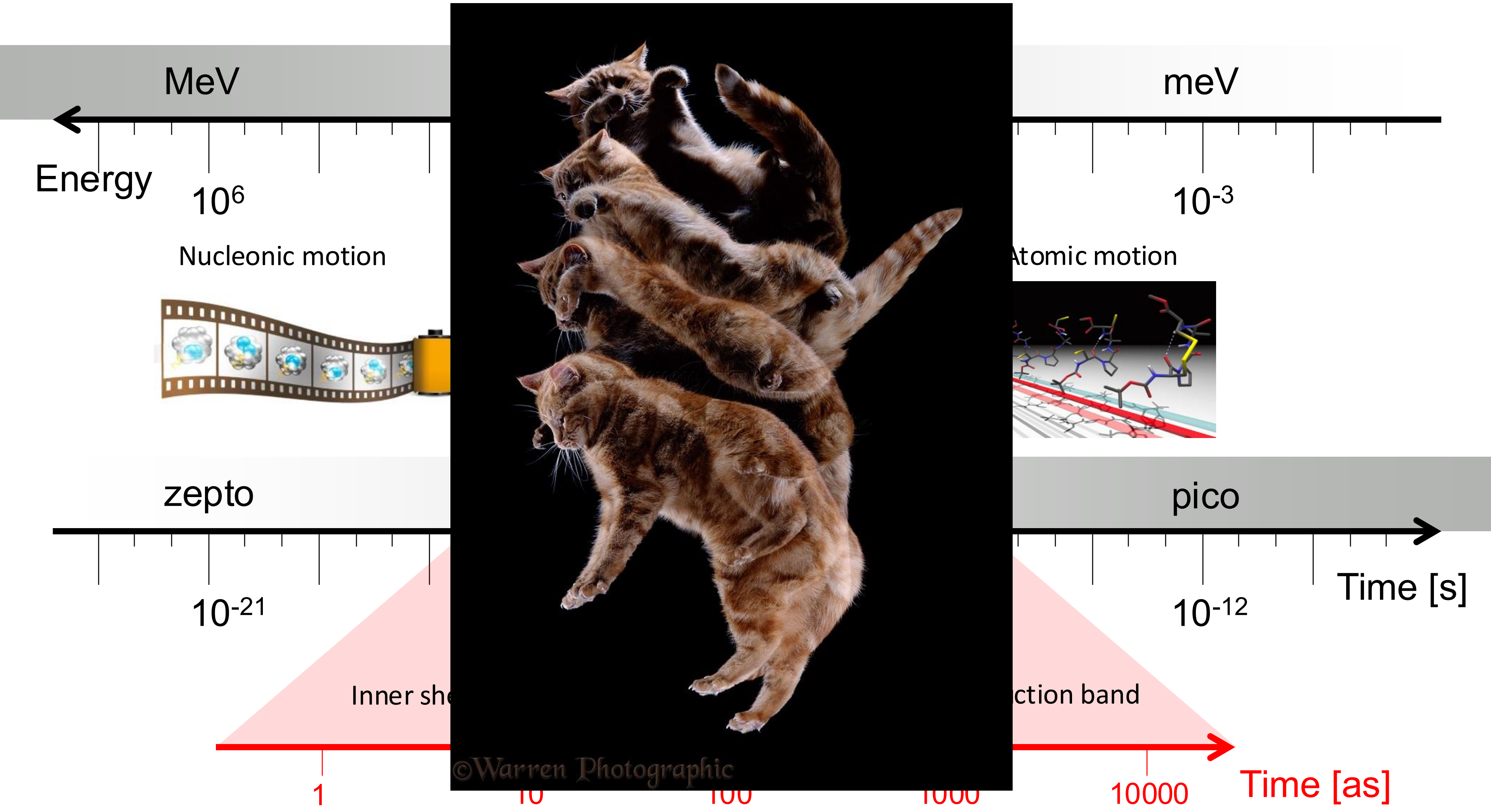

Outline

- **Attosecond pulse generation**
- **Charge migration: A route to attochemistry**
- **Photoemission Delays and Nanoplasmonics**

Time-resolved measurement: "pump & probe"

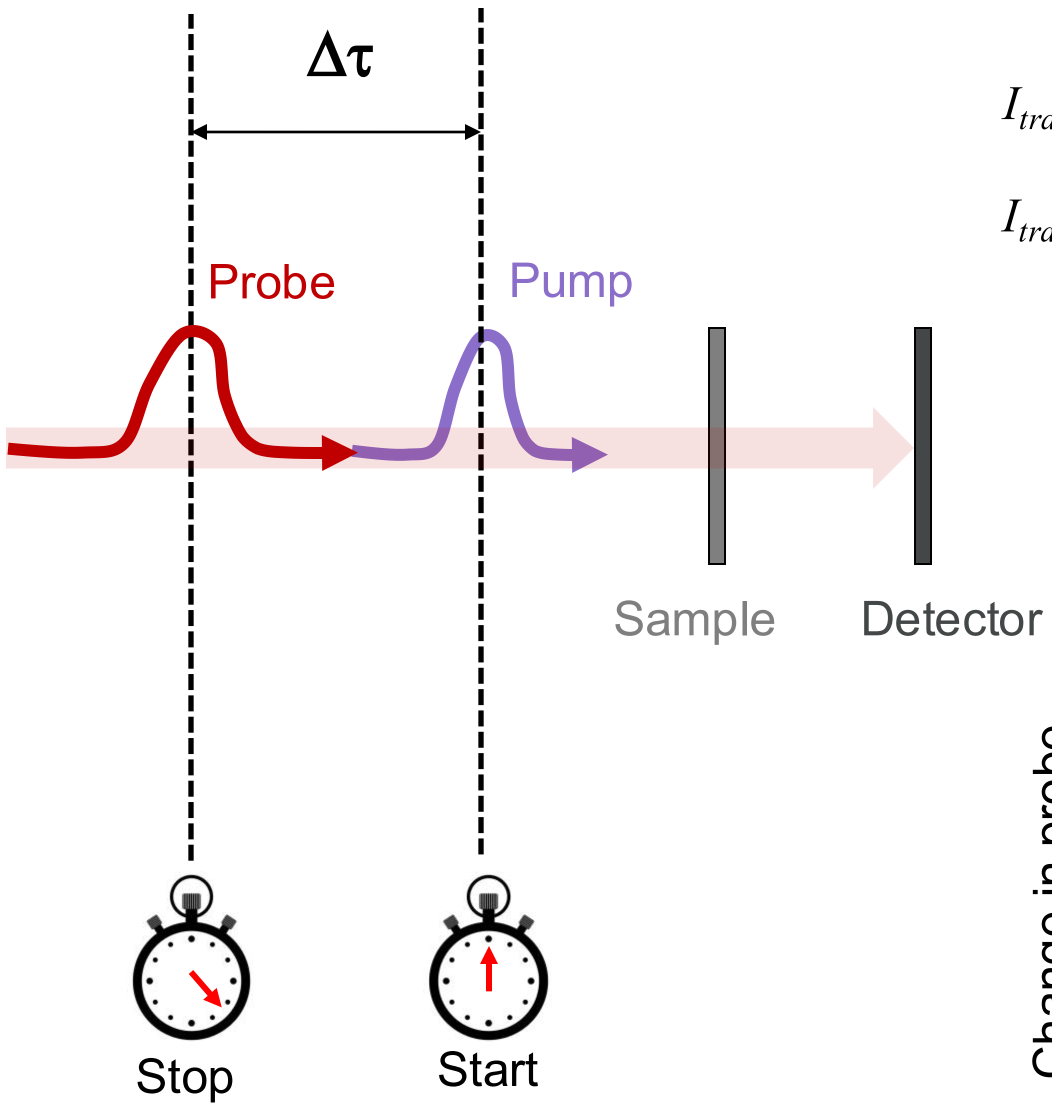

$$I_{transmitted} = I_{incident} \exp\{-\alpha_0 L\}$$

$$I_{transmitted}(\tau) = I_{incident} \exp\{-[\alpha_0 - \Delta\alpha(\tau)]L\}$$

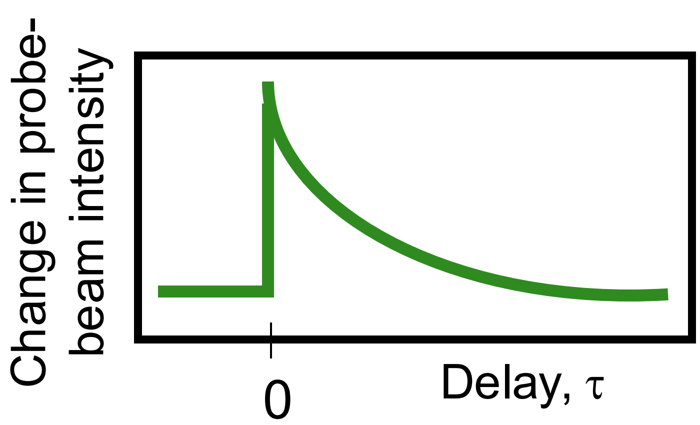

Ultrashort laser pulses: a limit in pulse duration imposed by carrier wavelength

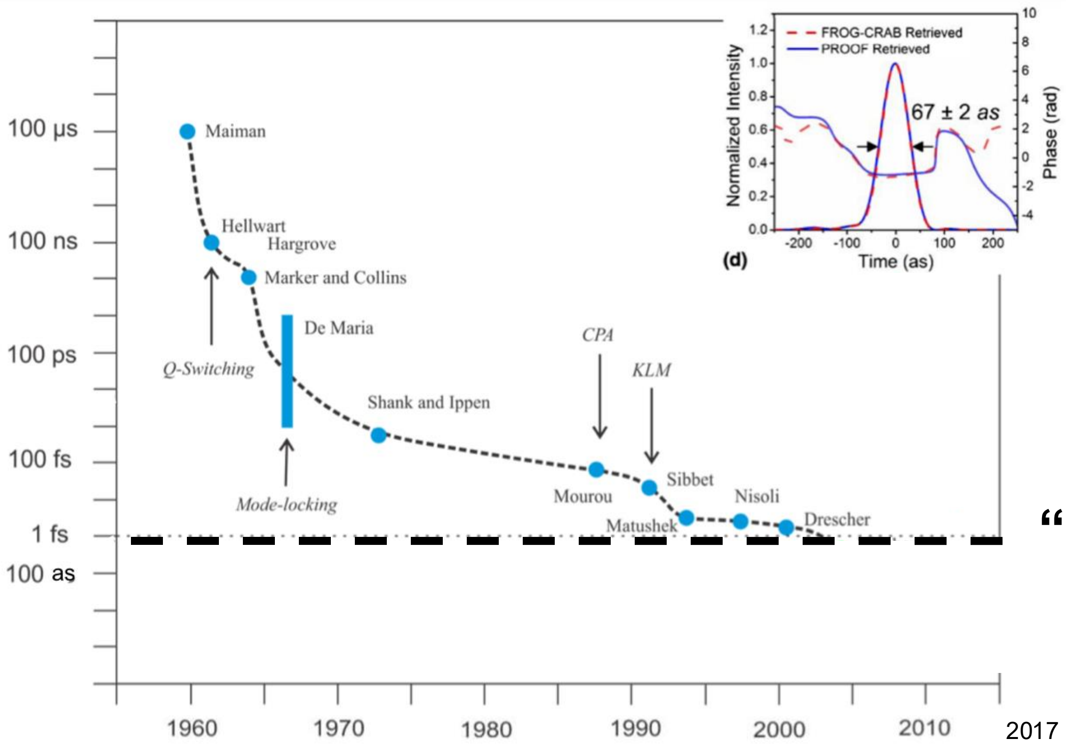

From Ursula Keller, Lecture notes "Ultrafast Lasers", ETH Zürich

Femtosecond pulses can be produced by conventional lasers

"Femtosecond barrier"

The 0-fs pulse

Wayne Knox
University of Rochester

Observation of the 0-fs pulse

By W.H. Knox, R.S. Knox, J.F. Hoose, and R.N. Zare

The quest for the world's shortest laser pulse has led to a remarkable pace of development in ultrafast laser technology. Although pulses of only a few cycles duration have been made, clearly the observation of a 0-fs pulse would represent a key result in this field (see Fig. 1). In most experiments, a 100-fs pulse is amplified and passed through a nonlinear medium, generally a simple single-mode silica optical fiber. The resulting nonlinear propagation creates a large bandwidth increase, and, with careful control of subsequent optical phases, significant compression ratios have been obtained. A simple linear extrapolation predicted that continued progress should result in an important milestone (dashed line): the pulsewidth should have gone to zero in late 1986 and become negative in 1987. Incorporation of prisms have produced at best 6-fs (three-cycle) pulses.

We show that the reason for this pause in history has been the choice of nonlinear medium. Single-mode fused silica fibers are not capable of generating enough bandwidth to approach the 0-fs limit and beyond with realizable intensities. Our new nonlinear medium consists of a short length (1–10 mm) of zirconium encrusted high-T_c superconductor microcrystallite doped neodymium aluminate fiber maintained near the superconducting transition by a liquid nitrogen cooled cryostat with optical access ports. A strong pulsed magnetic field parallel to the fiber axis is synchronized with the laser, providing 40–80 T peak field strength at 8 kHz repetition rate. We study the pulse evolution as a function of propagation distance and record conventional auto correlations.

Figure 2 shows our results. At 3 mm, note that the pulse FWHM actually goes to zero, and with longer propagation distance continues to go negative. This results, we believe, from the re-entrant behavior of the effective nonlinearity due to local-field effects in our microcrystallites. It is not clear how the nonlinear response exactly manages to modulate the dielectric function in such a way as to effect essentially a "wormhole" for passage of phase (not amplitude) in-

We tried to measure the power spectrum for the case closest to the 0-fs pulse. Uncertainty relations might appear to require an infinite bandwidth for a 0-fs pulse. Interestingly, the spectrum of the 0-fs pulse reveals an important feature of the 0-fs pulses that is not true of the 0-pi pulse. A 0-pi pulse has no area, but has energy. A 0-fs pulse has area, but no energy. This can easily be understood—the energy is just equal to the peak power

body's pulses must be getting longer.

W.H. Knox of AT&T Bell Laboratories, R.S. Knox of the University of Rochester's Department of Physics and Astronomy, J.F. Hoose of Milton Roy Inc., and R.N. Zare of Stanford's Department of Chemistry carried out this work especially for the April issue of *Optics & Photonics News*.

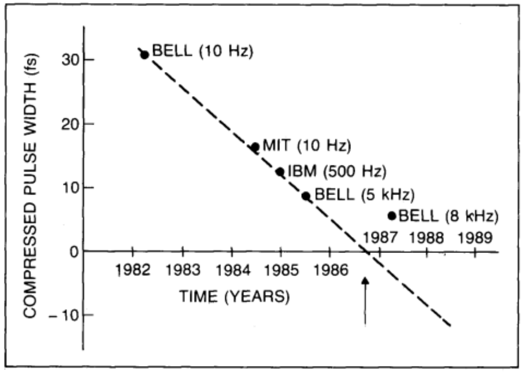

FIGURE 1. Evolution of pulse compression. The dashed line shows that in 1985 the 0-fs pulse was predicted to occur in late 1986. New nonlinear materials now allow us to attain this limit and beyond. Applications of large-negative-pulsewidth optical pulses should be abundant.

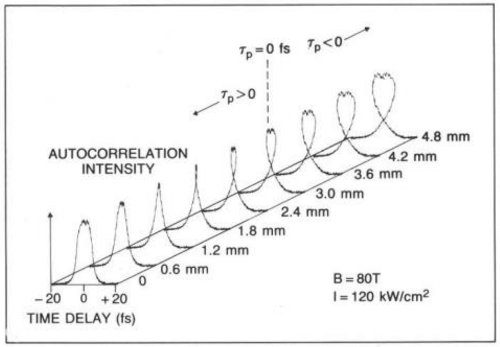

FIGURE 2. Autocorrelations of compressed pulses as a function of fiber length. We clearly observe the transition from normal pulse compression to 0-fs compression and beyond to the negative limit. We cannot test the uncertainty principle because the 0-fs pulse has no energy.

We are investigating possible violations of thermodynamics. Somebody's pulses must be getting longer.

Ultrashort laser pulses: a limit in pulse duration imposed by carrier wavelength

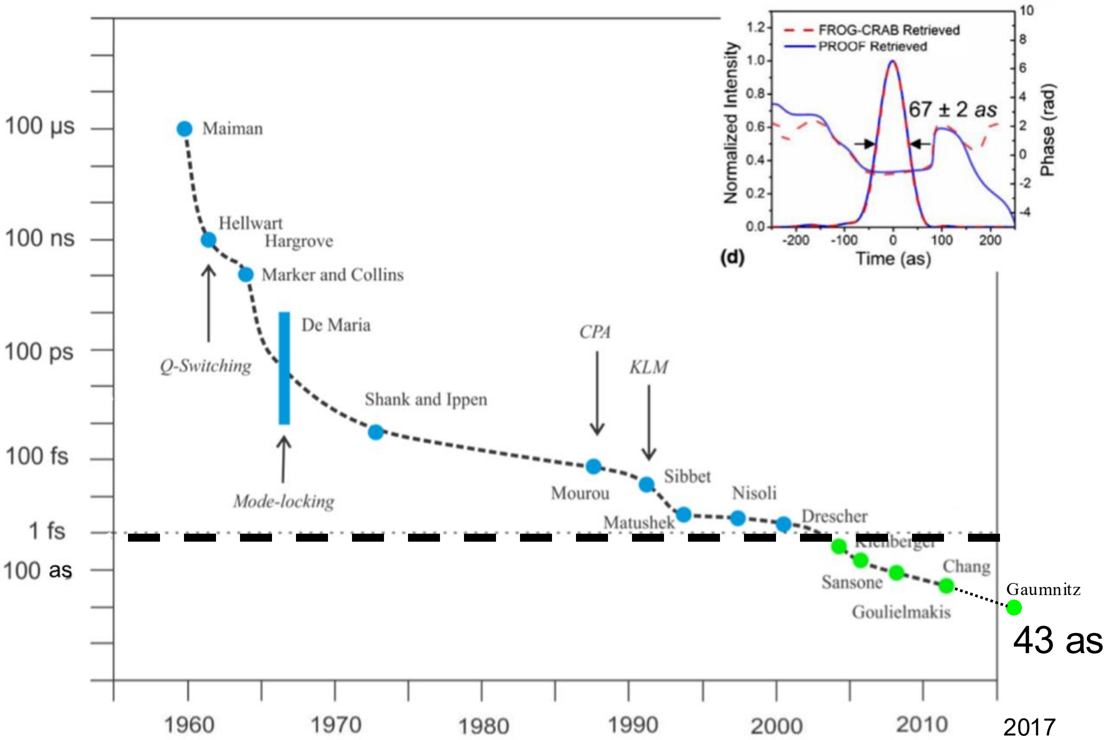

From Ursula Keller, Lecture notes "Ultrafast Lasers", ETH Zürich

Femtosecond pulses can be produced by conventional lasers

Attosecond pulses cannot be produced by conventional lasers: need for shorter wavelengths

Nonlinear optics: perturbative regime

$$P = \varepsilon_0 \left[\chi^{(1)} E + \chi^{(2)} E^2 + \chi^{(3)} E^3 + \ldots \right]$$

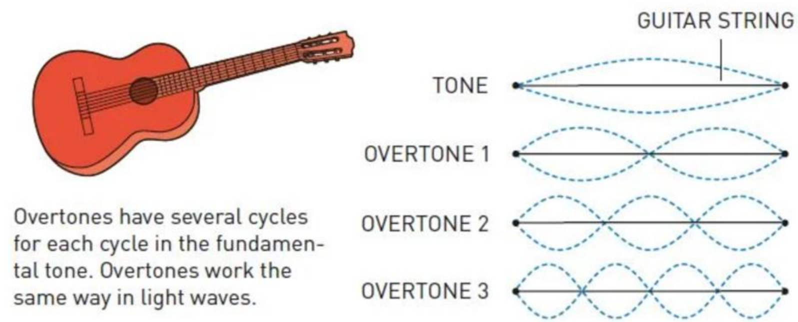

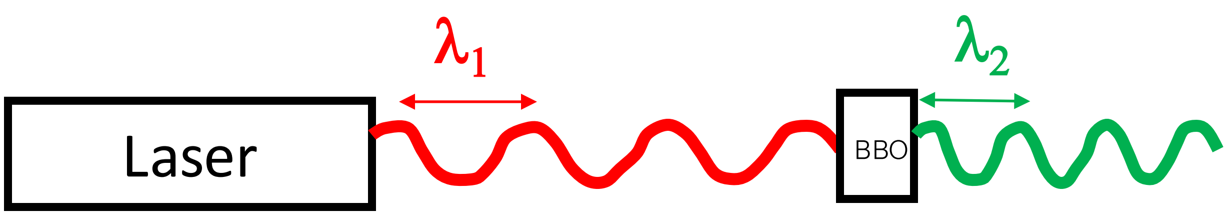

$\lambda_2 = \lambda_1 / 2$

Second Harmonic Generation (SHG)

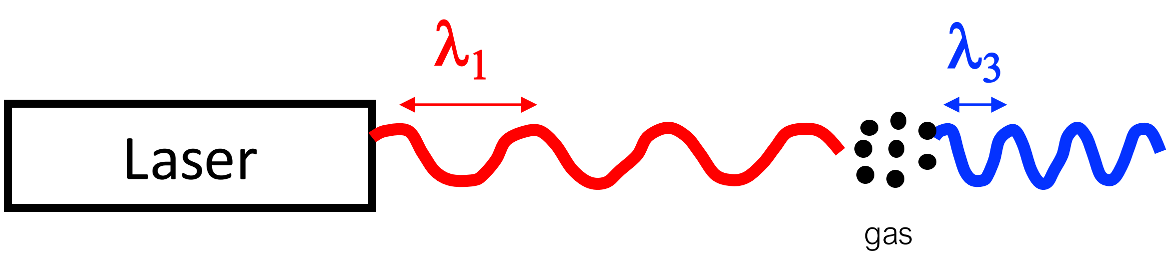

$\lambda_3 = \lambda_1 / 3$

Third Harmonic Generation (THG)

Extreme nonlinear optics: non-perturbative regime

I >10^{14} W/cm^2 → Highly non-perturbative interaction

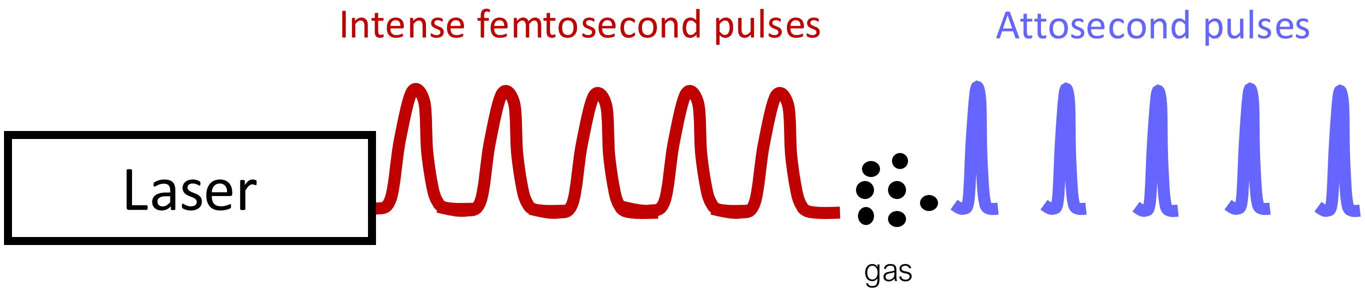

$\lambda_n = \lambda_1/n$

n = 7,9,11,13,…

Ill. Niklas Elmehed © Nobel Prize Outreach
Pierre Agostini
Prize share: 1/3

Ill. Niklas Elmehed © Nobel Prize Outreach
Ferenc Krausz
Prize share: 1/3

Ill. Niklas Elmehed © Nobel Prize Outreach
Anne L'Huillier
Prize share: 1/3

First observation of HHG

High-order Harmonic Generation - HHG

In the late 90's scientists observed frequency conversion of laser pulses to the XUV at orders incompatible with a perturbative multi-photon picture

Nonlinear optics was so far discussed only as a small perturbation of linear optics, giving rise to higher order terms

$$P = \varepsilon_0 \left[\chi^{(1)} E + \chi^{(2)} E^2 + \chi^{(3)} E^3 + \ldots \right]$$

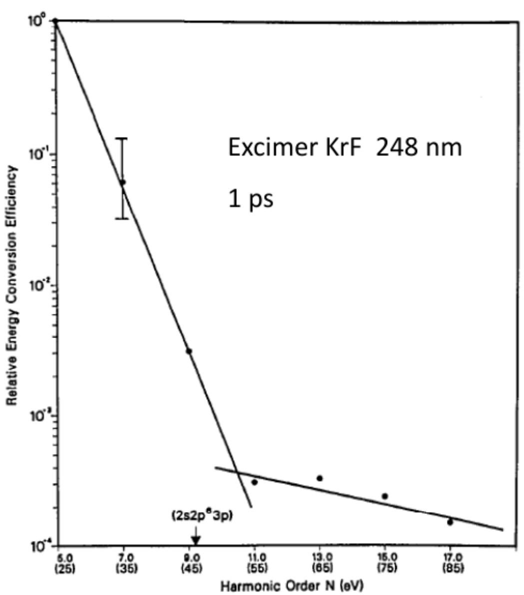

McPherson et al, JOSA B (1987)

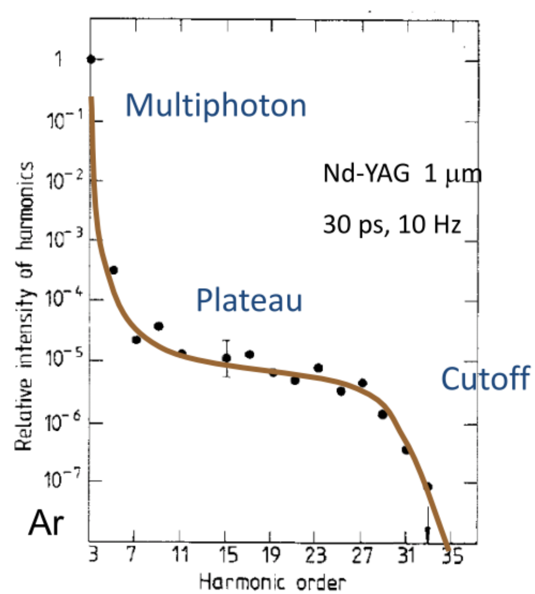

J Ferray et al, J. Phys. B (1988)

Ill. Niklas Elmehed © Nobel Prize Outreach

Anne L'Huillier

Prize share: 1/3

High-order Harmonic Generation

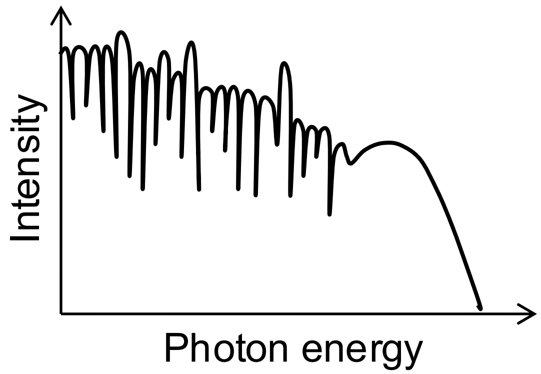

Three-step model

1. Tunnel ionization
2. Acceleration
3. Recollision

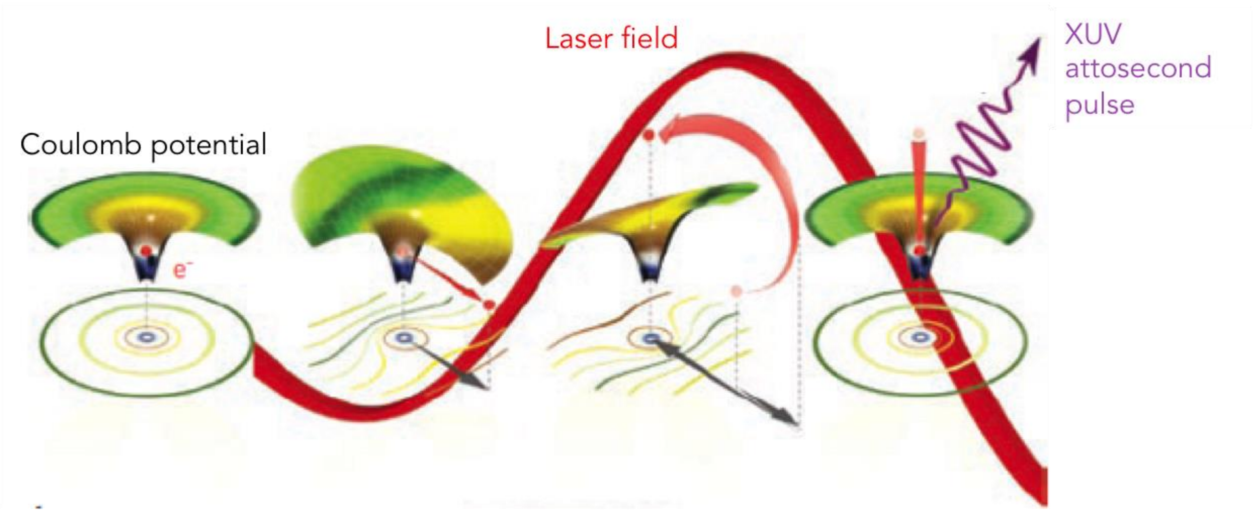

K.J. Schafer et al, Phys. Rev. Lett. 70, 1599 (1993)

P. B. Corkum, Phys. Rev. Lett. 71, 1994 (1993)

The attosecond pulse train

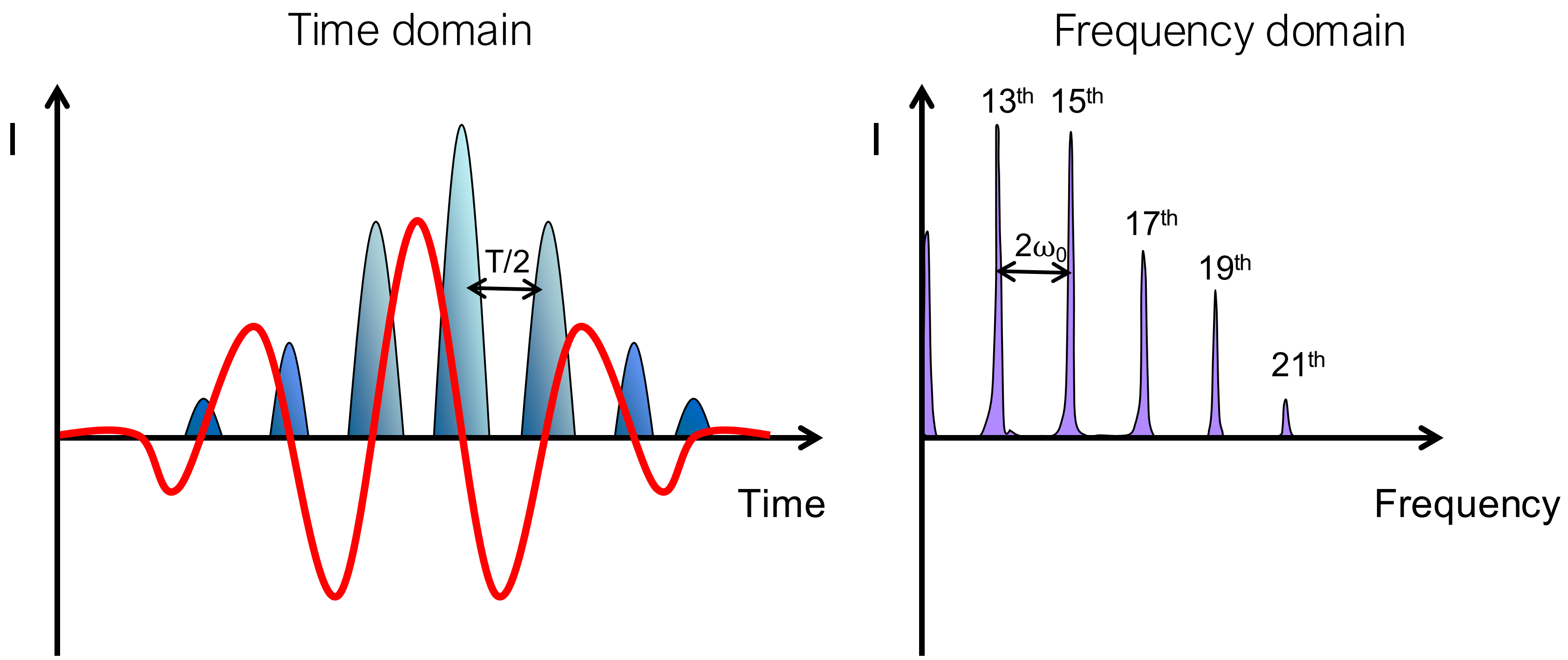

HHG every half cycle of the driving laser: attosecond pulse train

The interference between attosecond pulses separated T/2 gives rise to odd order harmonics of the fundamental frequency (spaced 2ω)

Isolated attosecond pulses

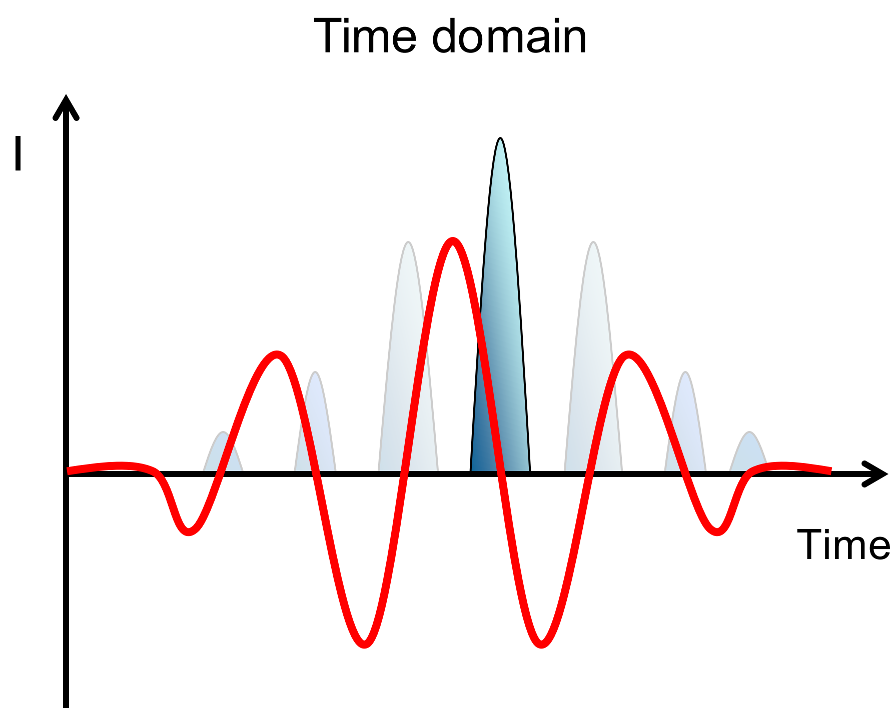

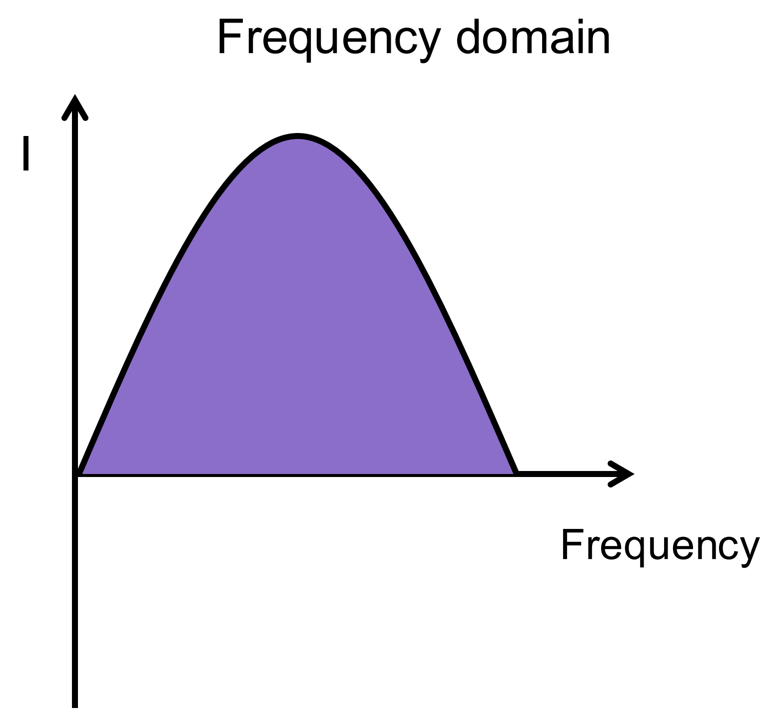

Spectral and temporal gating methods on HHG enable the generation of an isolated attosecond pulse

Shortest attosecond pulse 43 as!

T Gaumnitz et al, Optics Express 25 (2017)

First measurement of isolated attosecond pulses

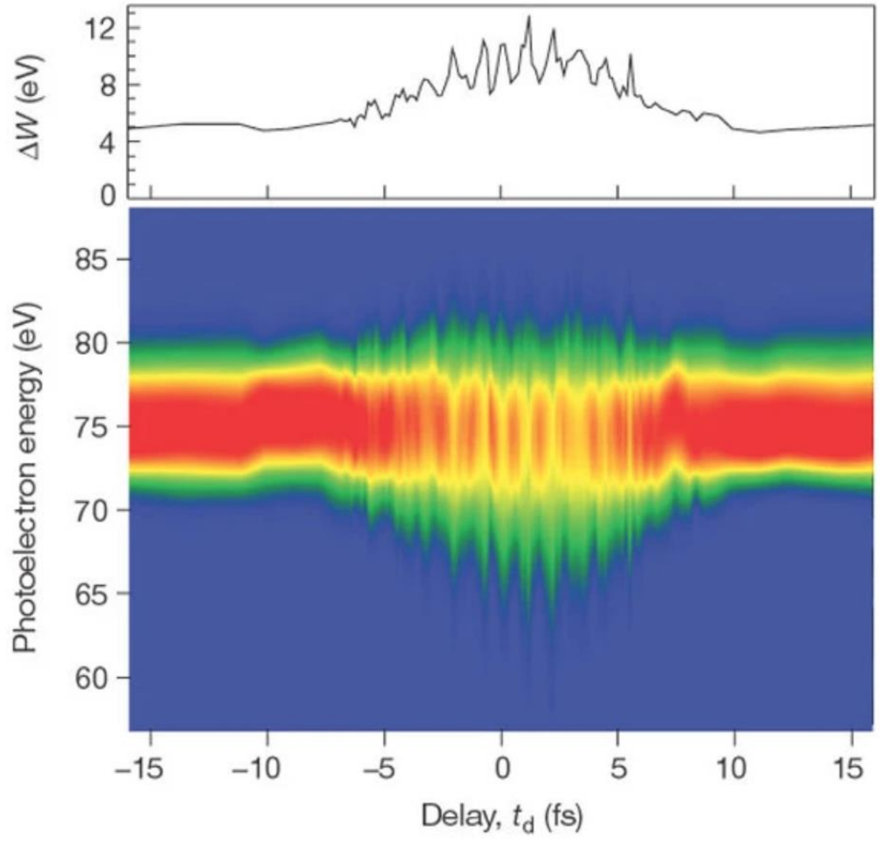

Ill. Niklas Elmehed © Nobel Prize Outreach

Ferenc Krausz

Prize share: 1/3

Hentschel, M. et al. Attosecond metrology. Nature 414, 509–513 (2001)

First temporal gating approaches

Polarization gating

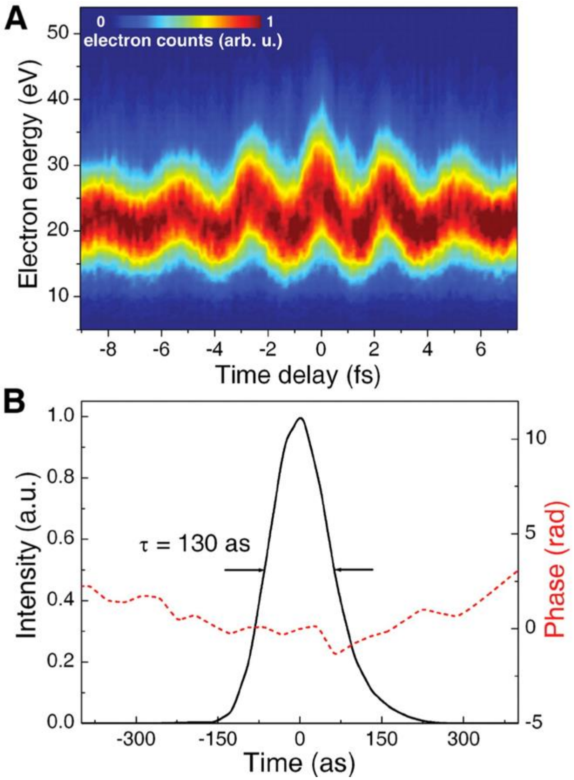

G. Sansone et al., Science 314, 443 (2006)

Ionization gating

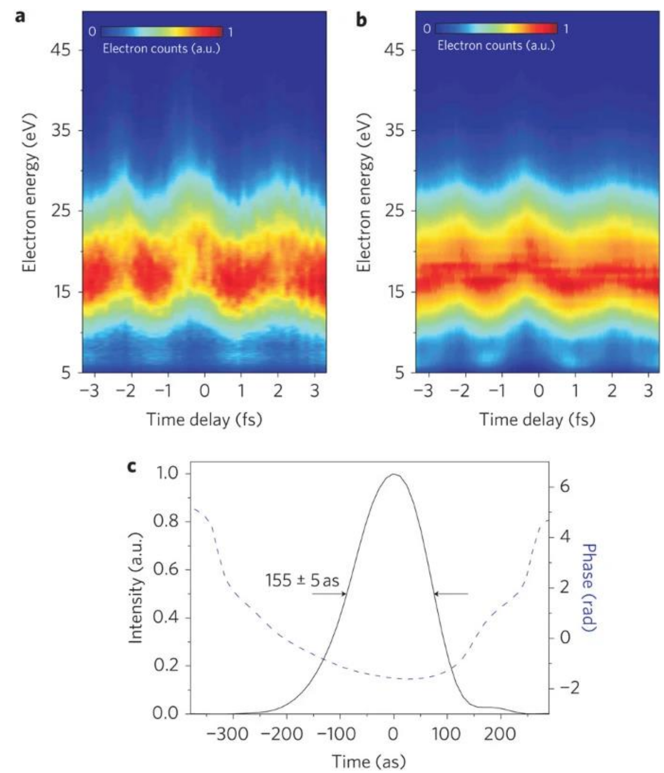

Ferrari, F., Calegari, F., et al. Nature Photon 4, 875–879 (2010)

Advancements in attosecond technology

Gating method (gas)	Central energy/ FWHM (eV)	Pulse duration/FT limit (as)	Pulse energy	Peak power (MW)	Characterization	Year/refs.
PG (Ne)	100/22	130/45	70 pJ	0.5	FROG-CRAB	2006/CNR-IFN/Italy[136]
AG (Ne)	83/28	80/75	0.5 nJ	6	FROG-CRAB	2008/MPQ/Germany[137]
IG (Xe)	25/8	155/130	9 nJ	60	FROG-CRAB	2010/CNR-IFN/Italy[138]
DOG (Ne)	100/40	67/16	N/A	N/A	PROOF	2012/UCF/USA[139]
Lighthouse (Ne)	50/35	(N/A)/47	N/A	N/A	N/A	2013/NRC/Canada[140]
TC (Xe)	30/7	500/(N/A)	1.3 µJ	2600	Autocorrelation	2013/RIKEN/Japan[141]
PG (Ne)	170/120	53/20	3 pJ	0.05	PROOF	2017/UCF/USA[36]
AG (Ne)	110/80	43/34	N/A	N/A	ML-VTGPA	2017/ETHZ/Switzerland[142]
AG (Ne)	250/100	<322/20	40 pJ	0.1	FROG-CRAB	2017/ICFO/Spain[26,143]
DOG (Ne)	150/100	305/(N/A)	0.3 nJ	1	Neural network	2019/UCF/USA[40]

Li, J., Lu, J., Chew, A. et al. Nat Commun 11, 2748 (2020)

- Attosecond sources deliver pulses in the mJ energy range
- Attosecond sources can cover the water window (200 – 500 eV)

Attosecond pump-probe setup

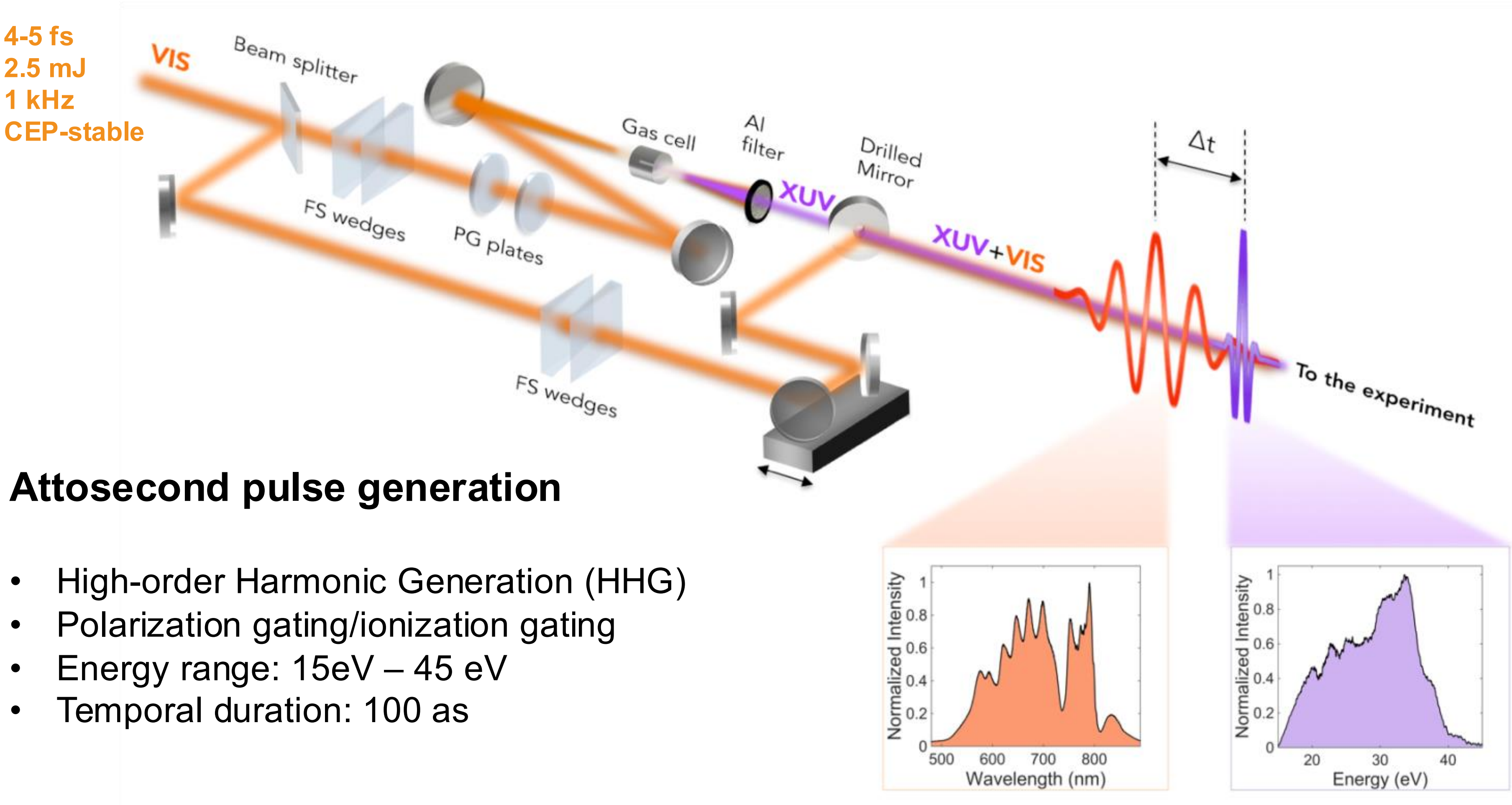

Attosecond pulse generation

- High-order Harmonic Generation (HHG)
- Polarization gating/ionization gating
- Energy range: 15eV – 45 eV
- Temporal duration: 100 as

F. Calegari et al., J. Phys. B: Atom. Mol. Opt. Phys. 49 , 062001 (2016)

Attosecond pump-probe setup + UV arm

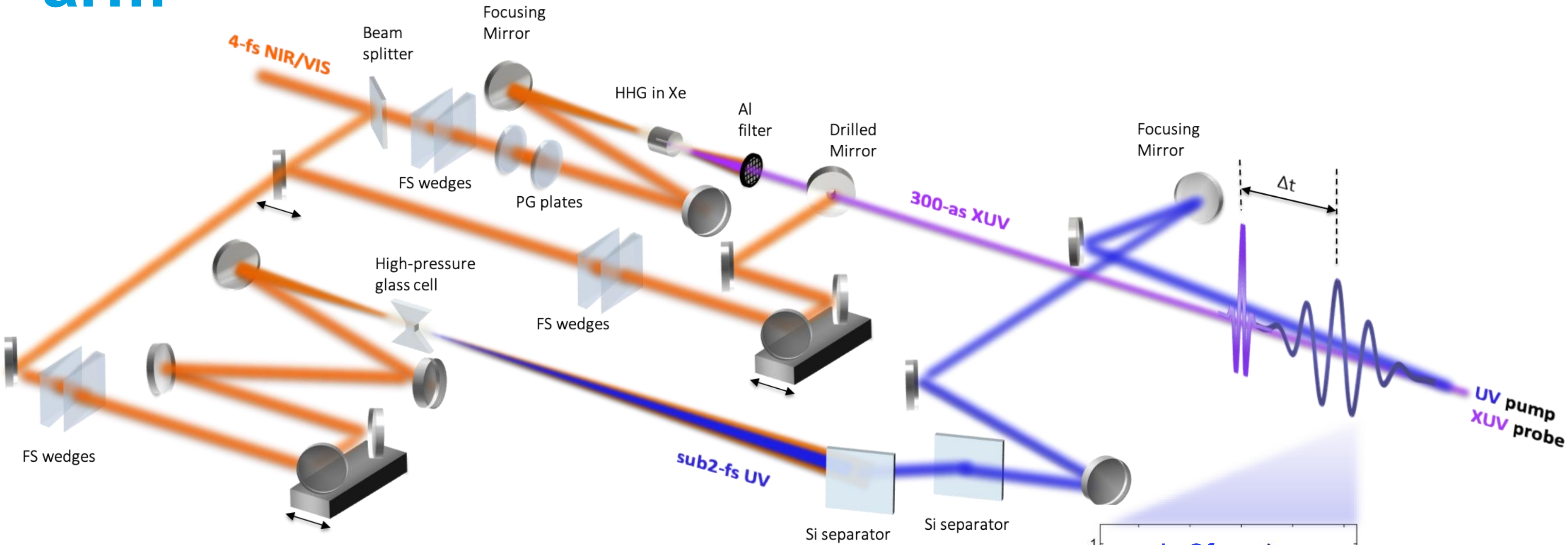

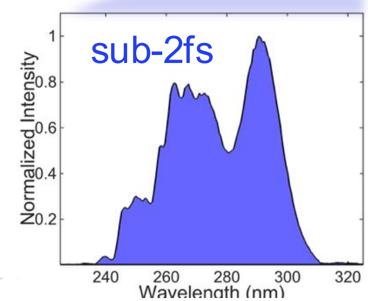

Combining XUV/soft-x attosecond pulses with sub-2fs UV pulses to explore **the electron time scale in neutral molecules**

V. Wanie et al., Rev. Sci. Instrum. 95, 083004 (2024)
M. Galli et al, Optics letters 44 (6), 1308-1311 (2019)
V. Wanie et al, J. Phys Photonics 6, 025005 (2023)

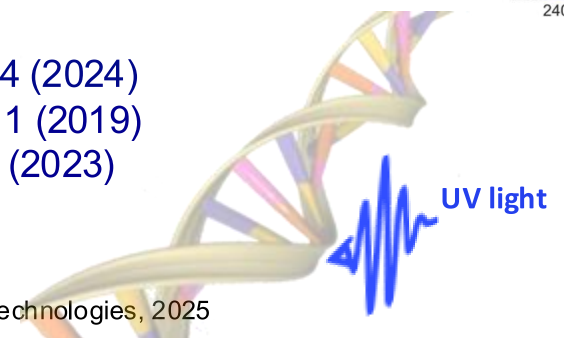

European Research Council
Established by the European Commission

Charge migration and attochemistry

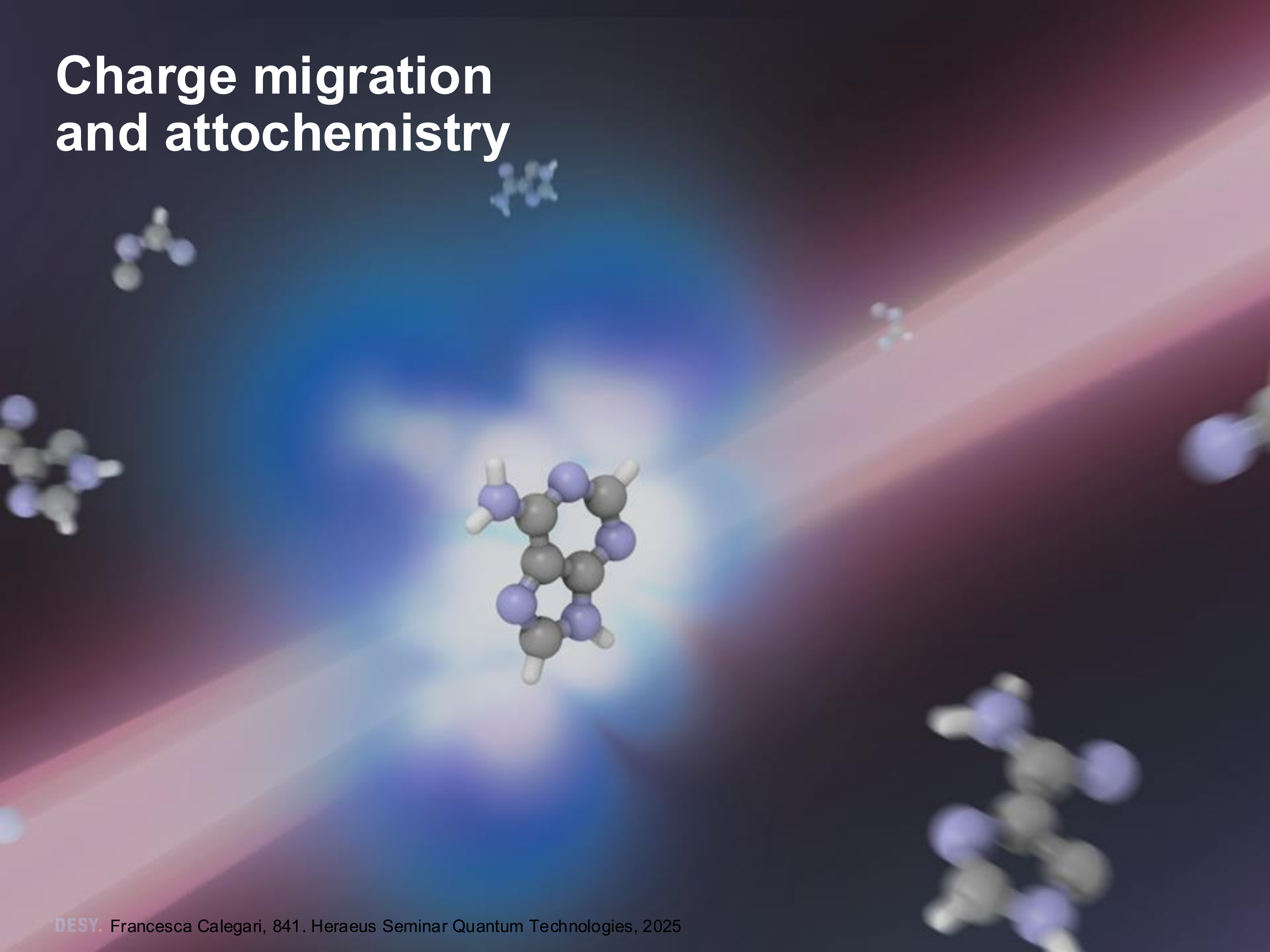

Femtochemistry: coherent control of chemistry by light

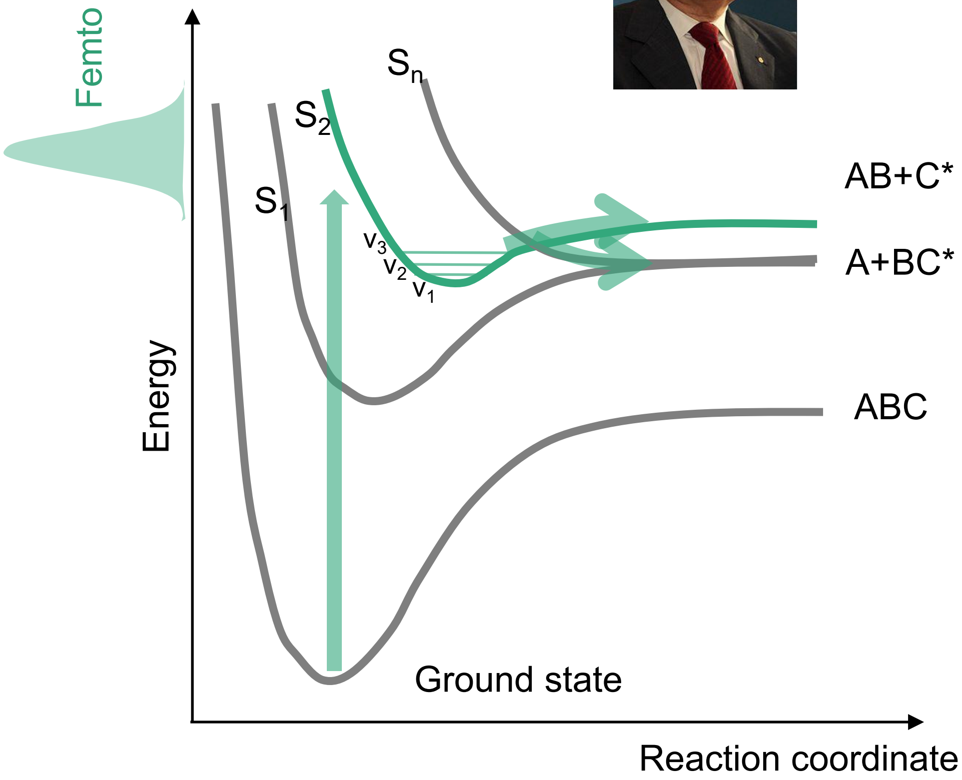

Classical forces on the atomic nuclei

Using **femtosecond pulses**:
The coherent excitation of a specific electronic state efficiently creates specific photoproducts.

Vibrational coherences can be populated.

$|\Psi\rangle = c_1\,|v_1\rangle + c_2\,|v_2\rangle \ldots + c_n\,|v_n\rangle$

A. H. Zewail, J. Phys. Chem. A, 104, 24, 5660 (2000)

Attochemistry: new quantum landscape

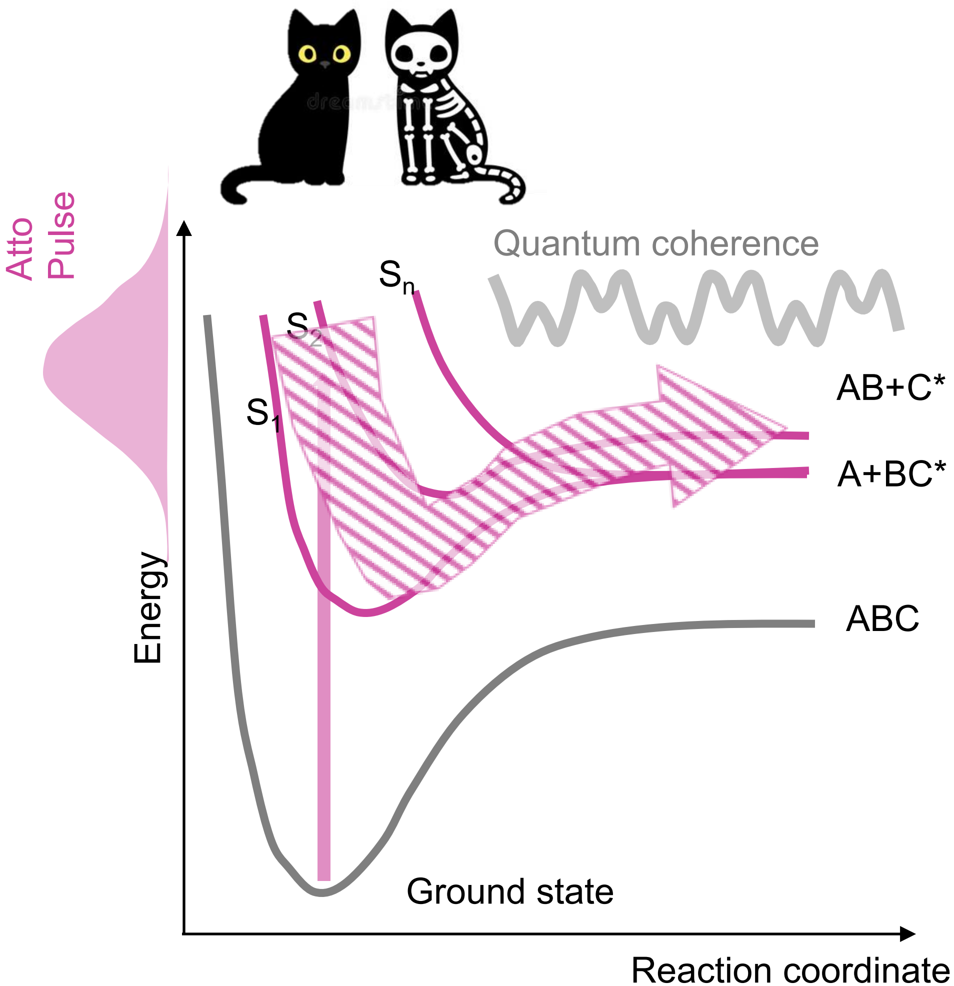

M. Cardosa-Gutierrez et al, J. Phys. B, 57 133501 (2024)

F. Calegari & F. Martin, Commun Chem 6, 184 (2023)

Quantum forces on the atomic nuclei

Using **attosecond pulses broadband and sudden excitation (fixed nuclei)**:

An electronic wavepacket (EWP) is created.

$|\Psi\rangle = c_1 |S_1\rangle + c_2 |S_2\rangle \ldots + c_n |S_n\rangle$

The quantum correlation between electron and nuclei creates new terms in the total force field → **shaping EWP allows to engineer the force.**

Charge directed reactivity!

Charge migration

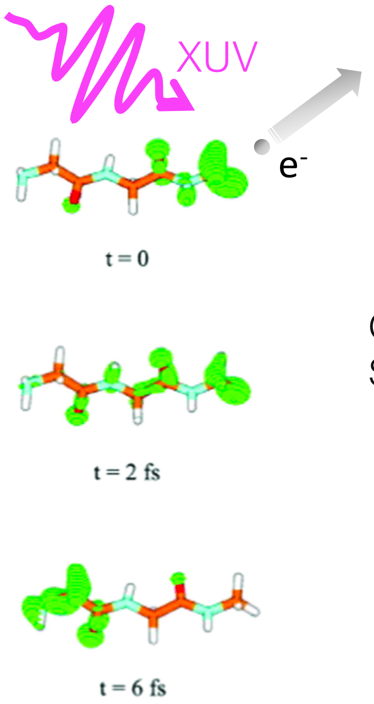

GlyGlyNHCH$_3$
Small peptide

Sudden ionization/electronic excitation leads to EWP creation and a non-stationary charge density distribution: **charge migration.**

- How can we initiate charge migration?
- How can we observe charge migration?
- Can we exert control on chemical reactivity?

S. Lünnemann et al., Chem. Phys. Lett. 450, 232 (2008)
L. Cederbaum et al, Chem. Phys. Lett. 307, 205 (1999)
F. Remacle, R. Levine, PNAS 103, 6793 (2006)
A. Kuleff, L. Cederbaum, Chem. Phys. 338, 320 (2007)

Detecting charge migration

Attosecond time resolved photofragmentation

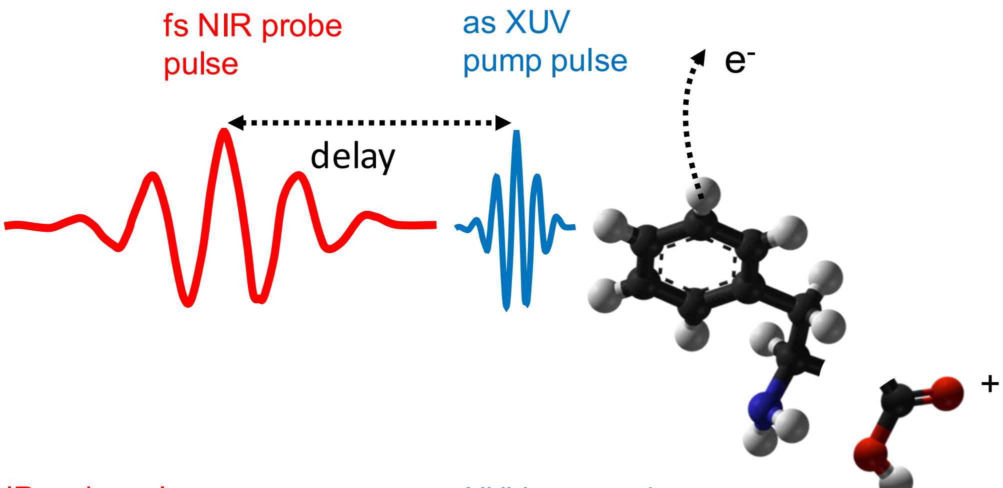

IR probe pulses:
Duration = 4 fs
Wavelength= 800nm
Intensity = 10^{12}-10^{13} W/cm^2
CEP-stable
Interferometer actively stabilized (RMS 10as)

XUV pump pulses:
HHG in Kripton
Polarisation gating
Duration = 200 as
Energy range = 17-45 eV
Pulse energy = few nJ

DETECTOR

MASS SPECTRUM

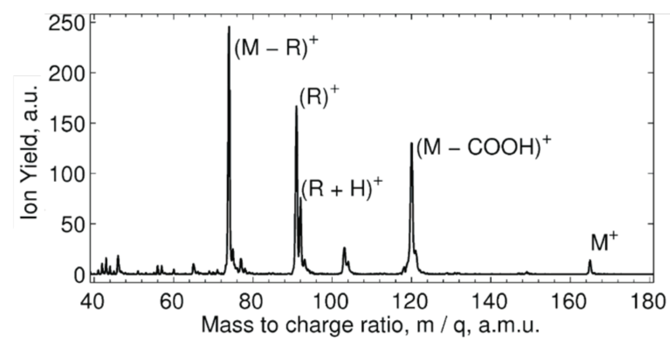

Charge migration in aromatic amino acids

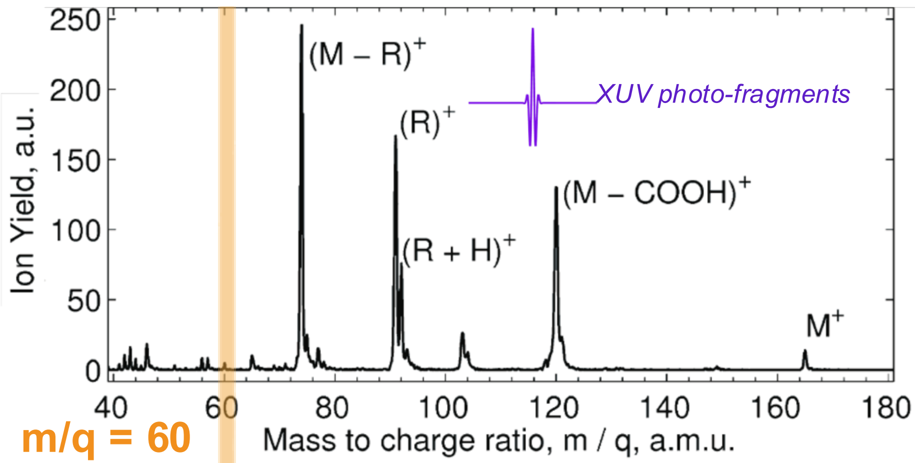

m/q = 60

PHENYLALANINE

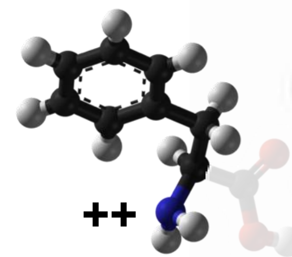

M+
Parent ion

(M – COOH)+
Immonium ion

R+
Side chain

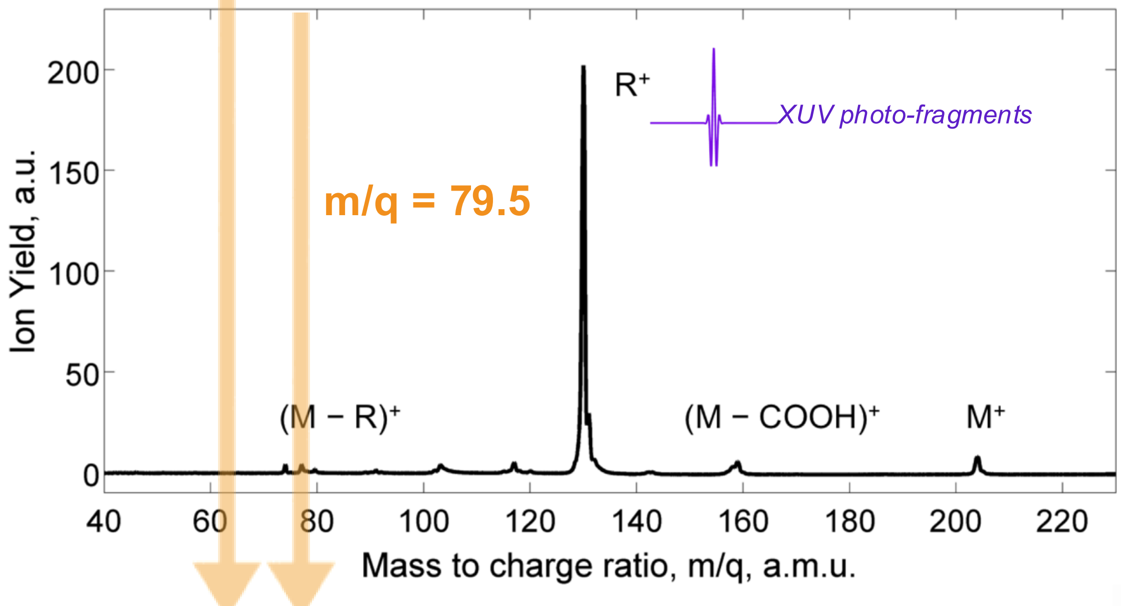

TRYPTOPHAN

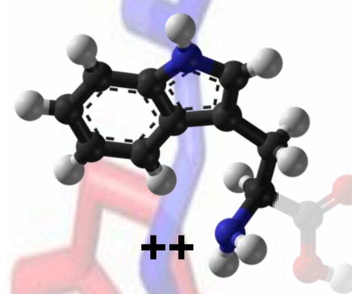

(M-COOH)++ = Doubly charged immonium ion

Charge migration in aromatic amino acids

Dication yield after subtraction of the 25-fs decay

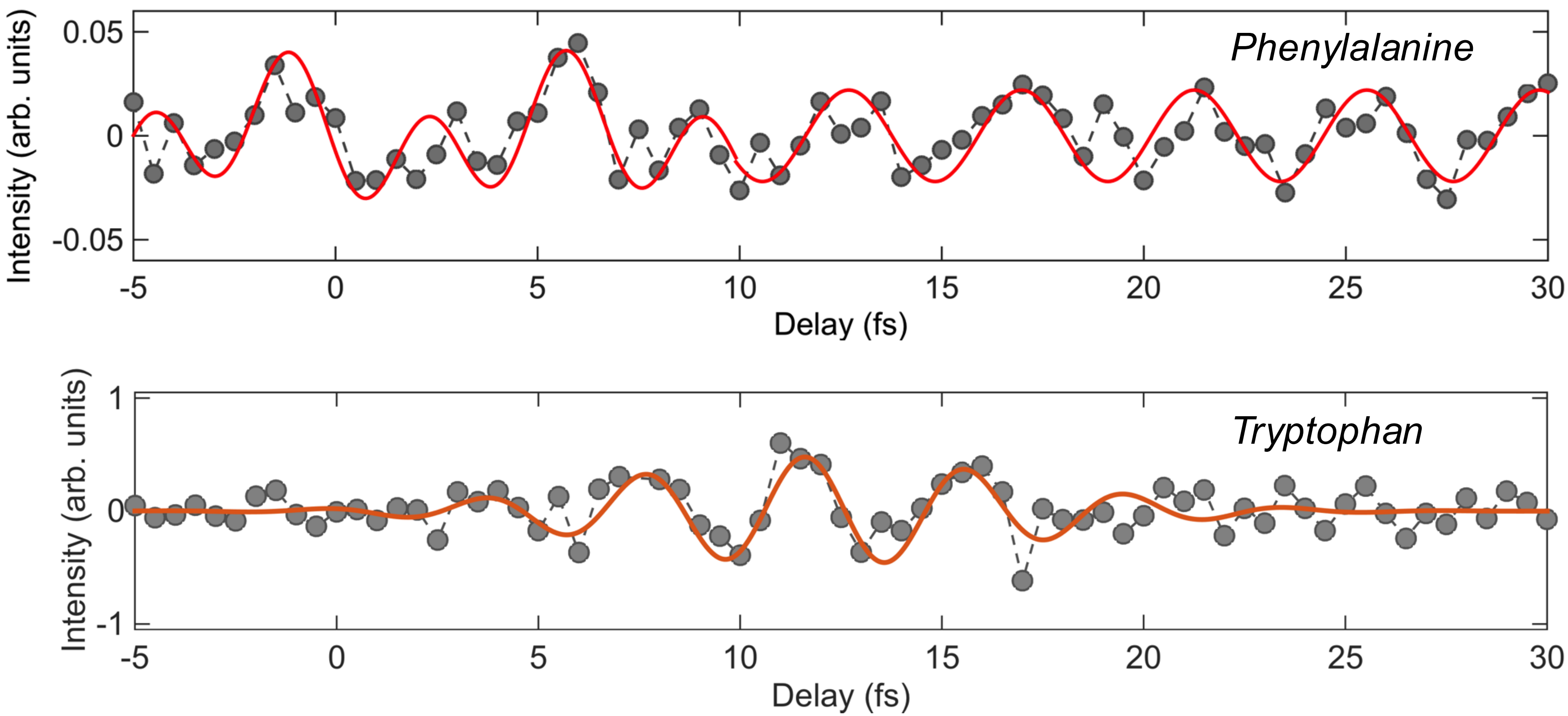

Sub 4.5 fs oscillations

F. Calegari et al., Science 346, 336 (2014)
M. Lara-Astiaso et al, The journal of physical chemistry letters 9 (16), 4570-4577, (2018)

Collaboration with M. Nisoli, Politecnico di Milano (Italy)

Charge migration in aromatic amino acids

An attosecond pulse is a broadband pulse!

→ Coherent superposition of a manifold of electronic states

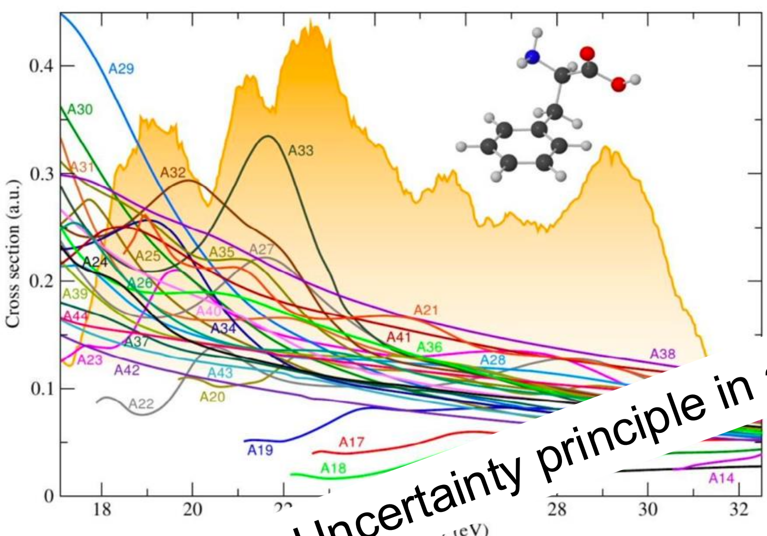

Uncertainty principle in action!

Phenylalanine

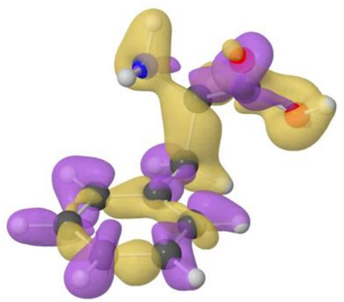

Tryptophan

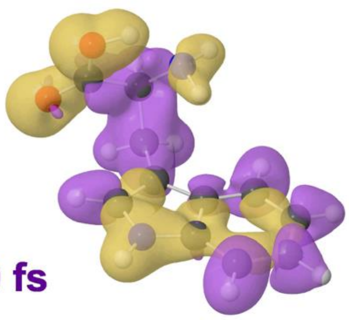

F. Calegari et al., Science 346, 336 (2014)

Collaboration with F. Martin, UAM (Madrid)

Attosecond pulses at XFELs

XLEAP

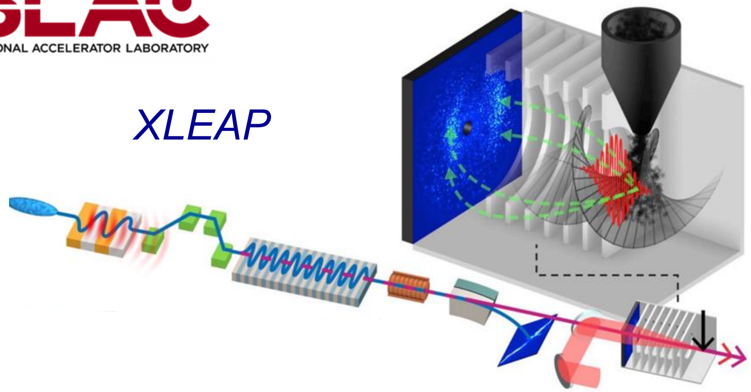

Duris, J. et al, Nat. Photonics 14, 30–36 (2020)

A. Marinelli

J. P. Cryan

Look at the dynamics site selectively with XAS

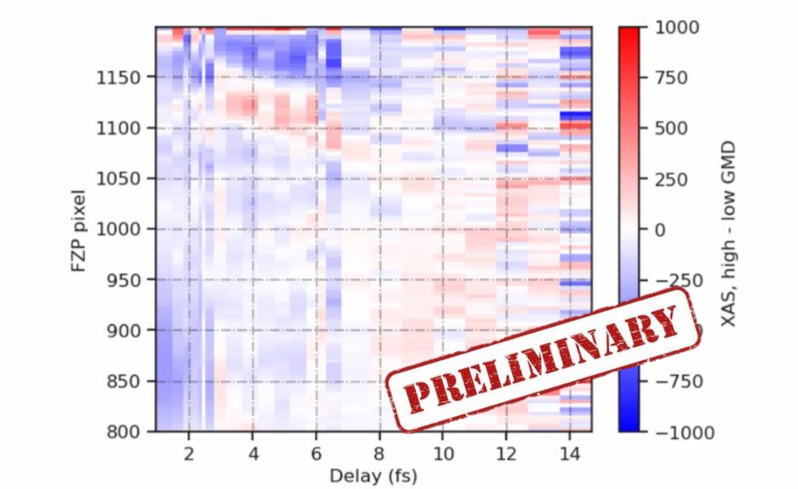

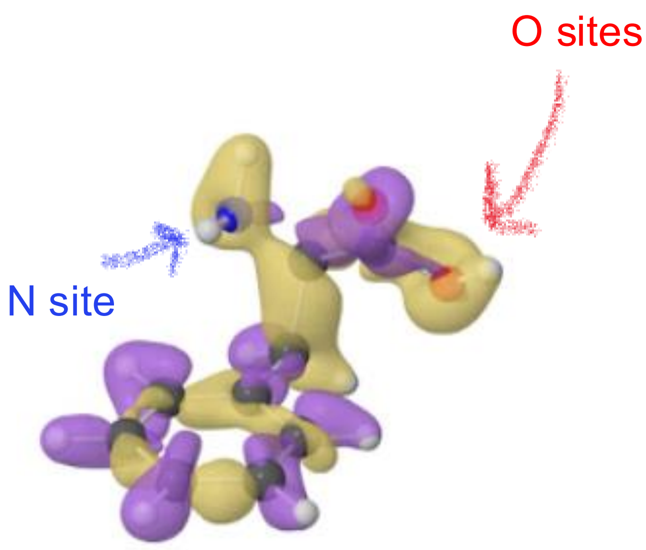

Chirality

Concept

- Non-superimposable mirror images
- Handedness defines the interaction with another chiral object

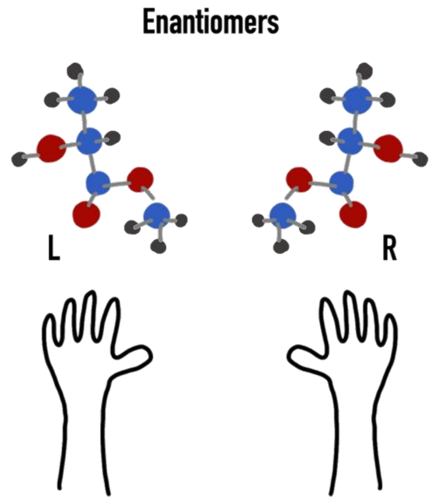

Chiral molecules = enantiomers

Chiral recognition

- Homochirality of all living organisms (l - amino acids)
- Pharmacology → healing vs toxic effect

l-methamphetamine

Nasal decongestant

d-methamphetamine

Recreational drug

Charge migration in neutral chiral molecules

Time-resolved PECD in methyl lactate

Methyl lactate

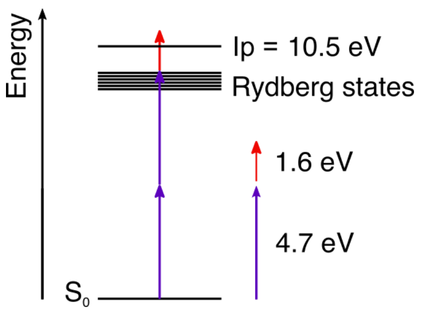

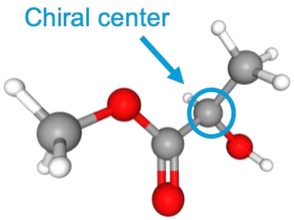

- The broadband UV pulse excites a coherent superposition of Rydberg states
- Photoelectron Circular Dichroism (PECD) can be used to detect the chiral response after electronic excitation

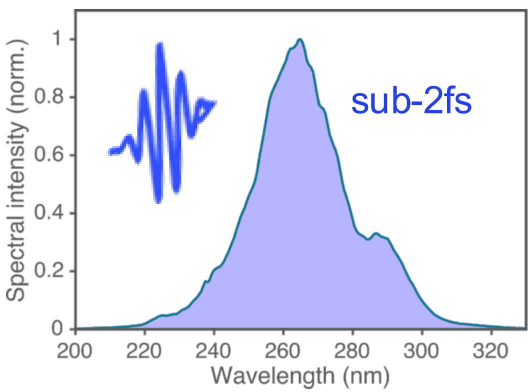

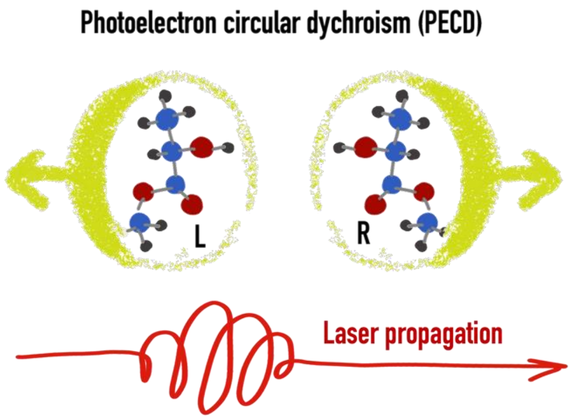

S. Beaulieu et al, Faraday Discuss., 194, 325 (2016)

Collaboration with Y. Mairesse and V. Blanchet, CELIA, Bordeaux

TR-PECD setup

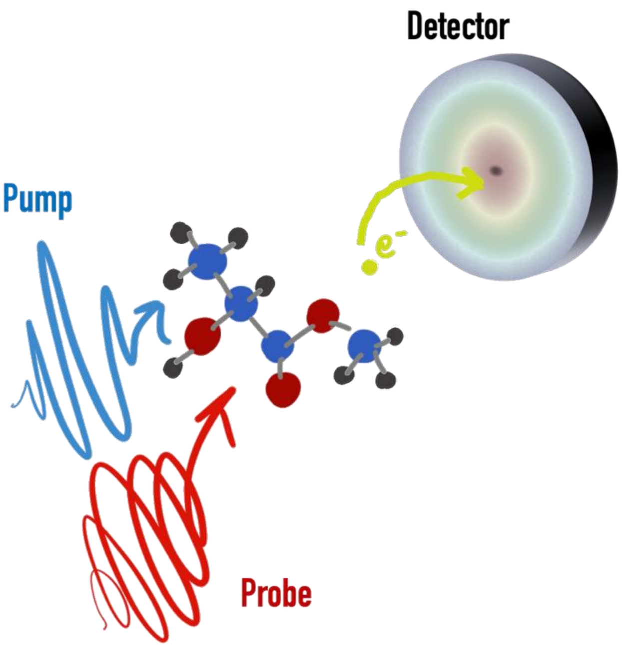

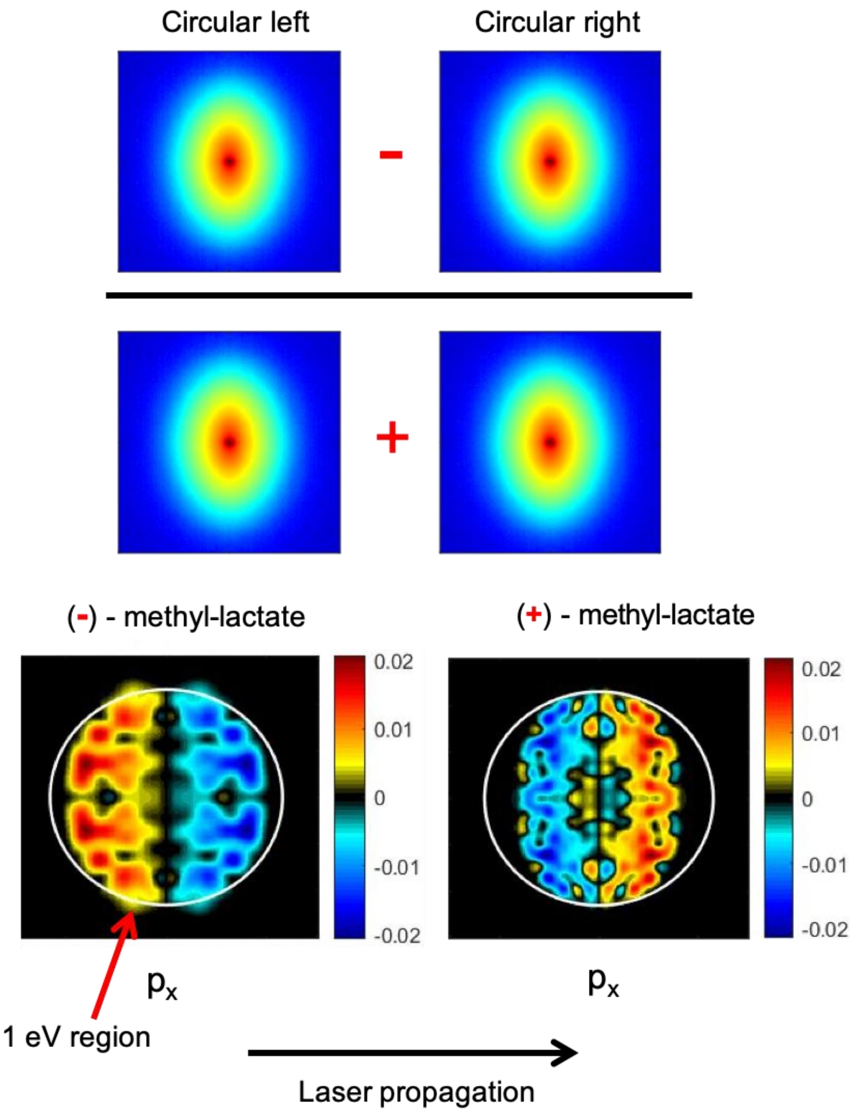

UV pump pulses:
Duration = sub-2fs
Energy range = 4-5 eV
Pulse energy = 100 nJ

IR probe pulses:
Duration = sub-5fs
Circularly polarized

Time-dependent PECD

Ultrafast inversion of PECD

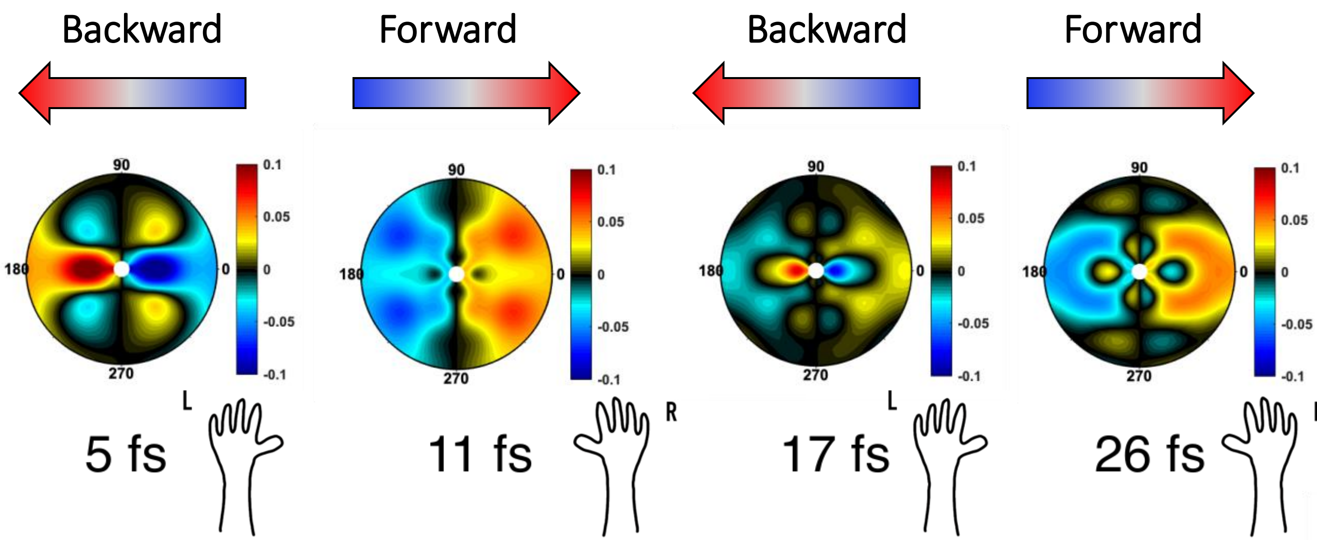

(S) - methyl-lactate

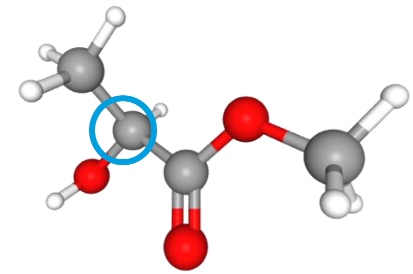

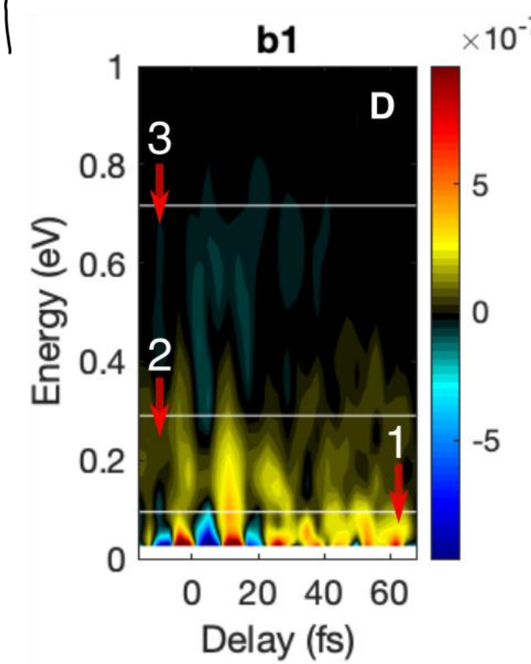

Energy-resolved fit of the angular distributions (p-Basex):

$$D(E,\theta) \approx \beta_0 \pm \beta_1 cos(\theta) + \beta_2 P_2(cos(\theta)) + ...$$

$$MP\text{-}PECD\ (E) = \frac{1}{\beta_0}\left(2\beta_1 - \frac{1}{2}\beta_3 + \frac{1}{4}\beta_5 - \frac{5}{32}\beta_7 + \ldots\right)$$

V. Wanie et al, Nature 630, 109 (2024)

Comparison with theory (TDDFT)

Time domain

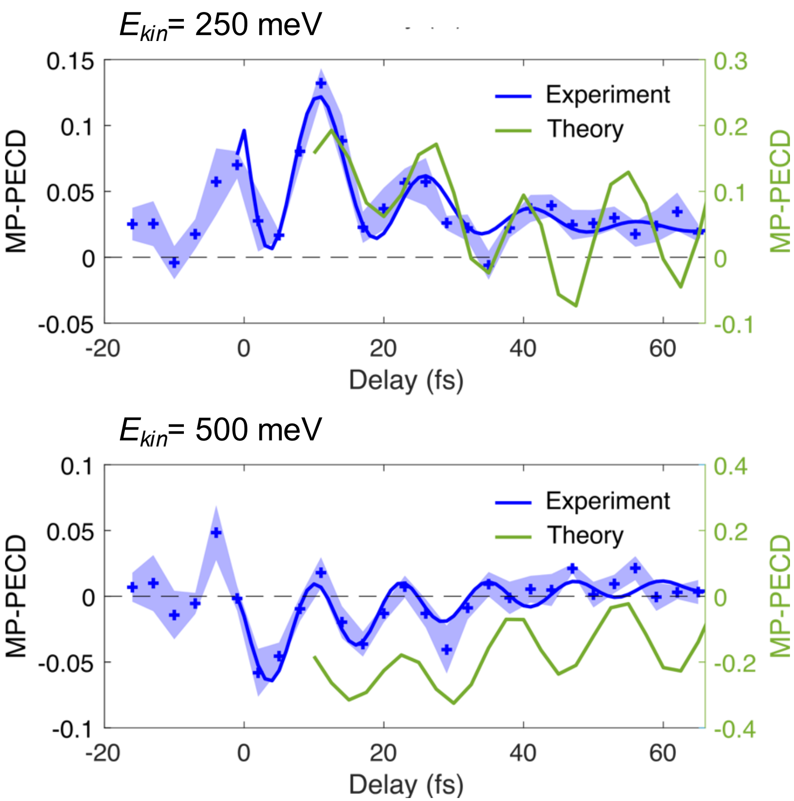

Frequency domain

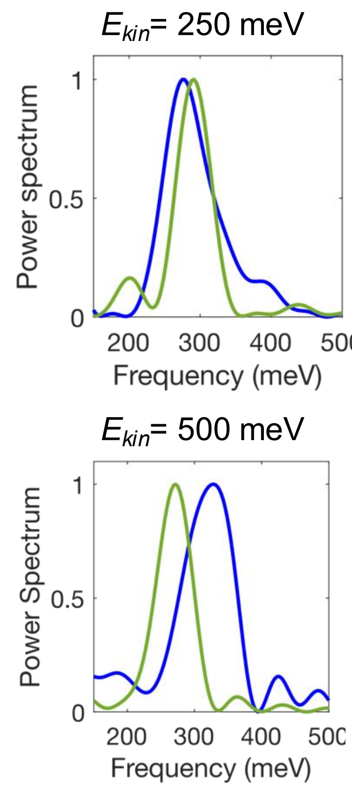

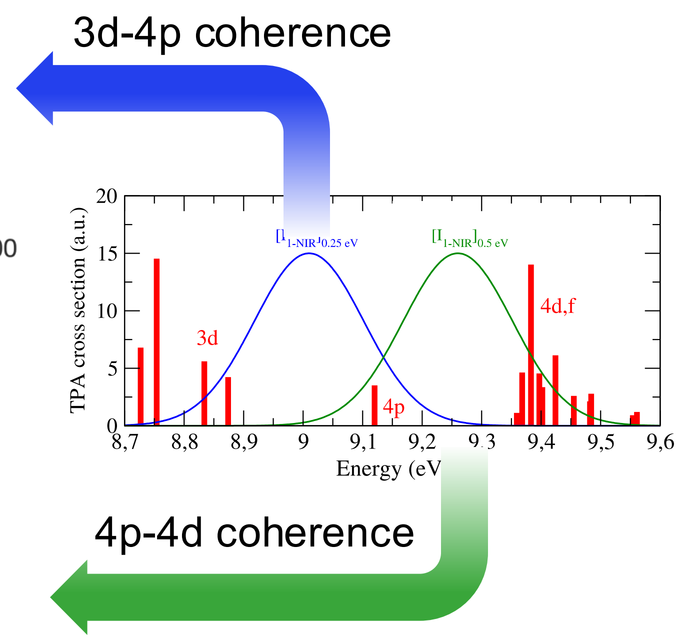

Coherent superposition of 3d-4p and 4p-4d,f states is responsible for the modulation of the PECD signal

Collaboration with B. Pons, CELIA, Bordeaux, N. Ben Amor and M.-C. Heitz, Université Paul Sabatier

Charge migration

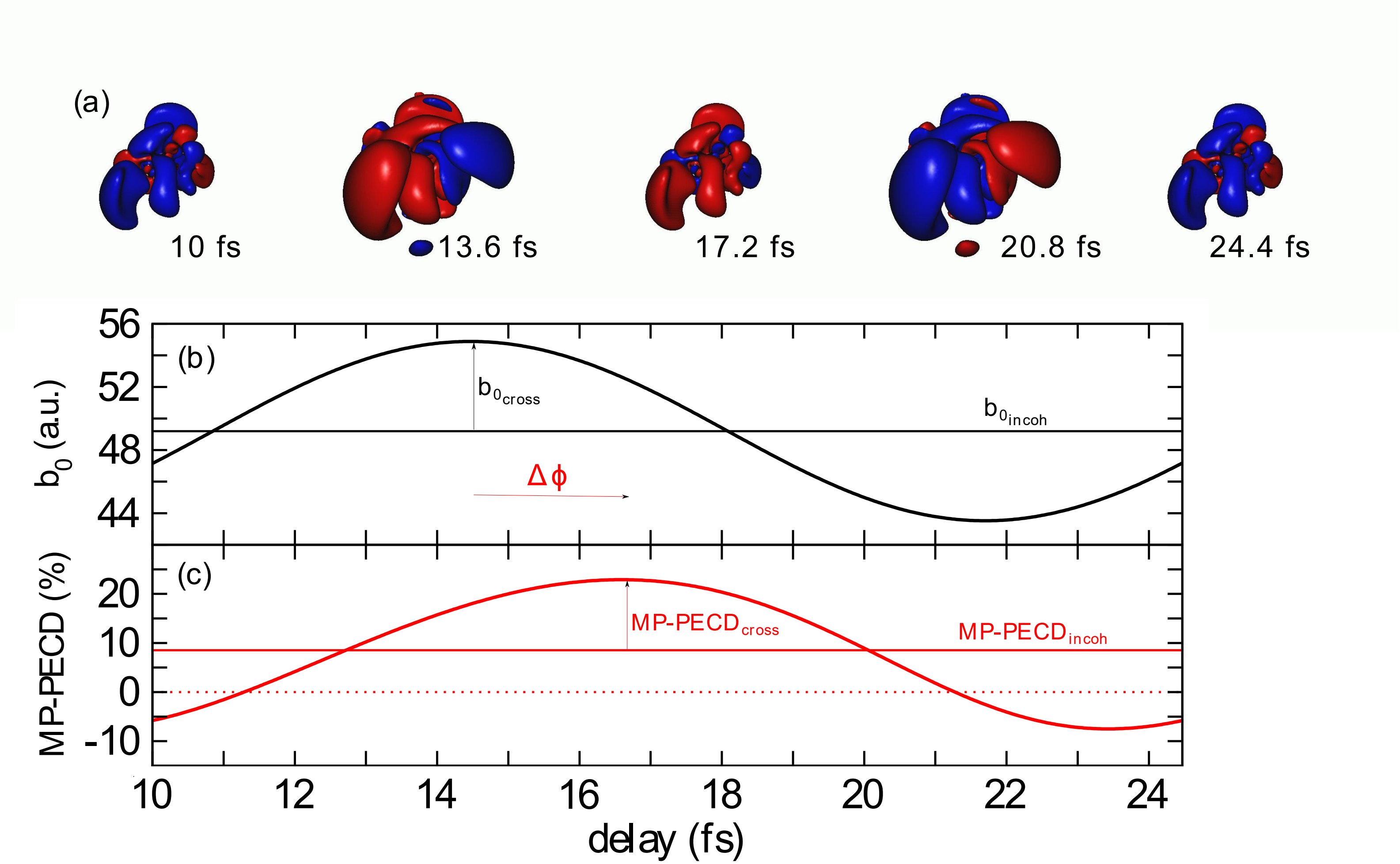

V. Wanie et al, Nature 630, 109 (2024)

Chiral currents

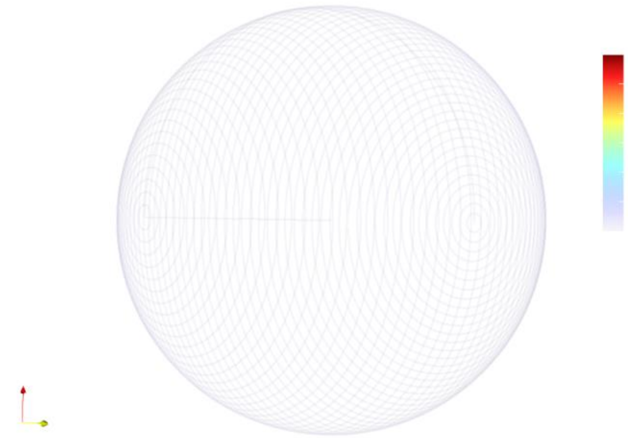

Charge migration results in chiral currents switching sign with the periodicity of the electronic beatings.

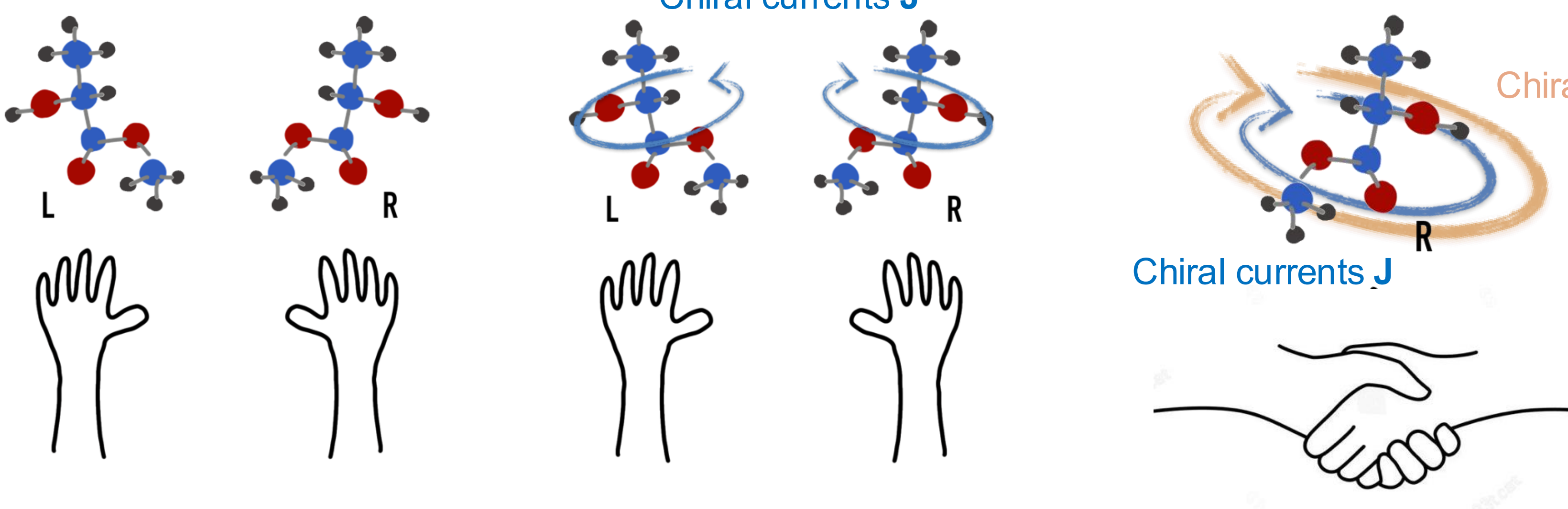

Transient chiral currents enable **control of enantio-selective interactions.**

Molecular orientation effects

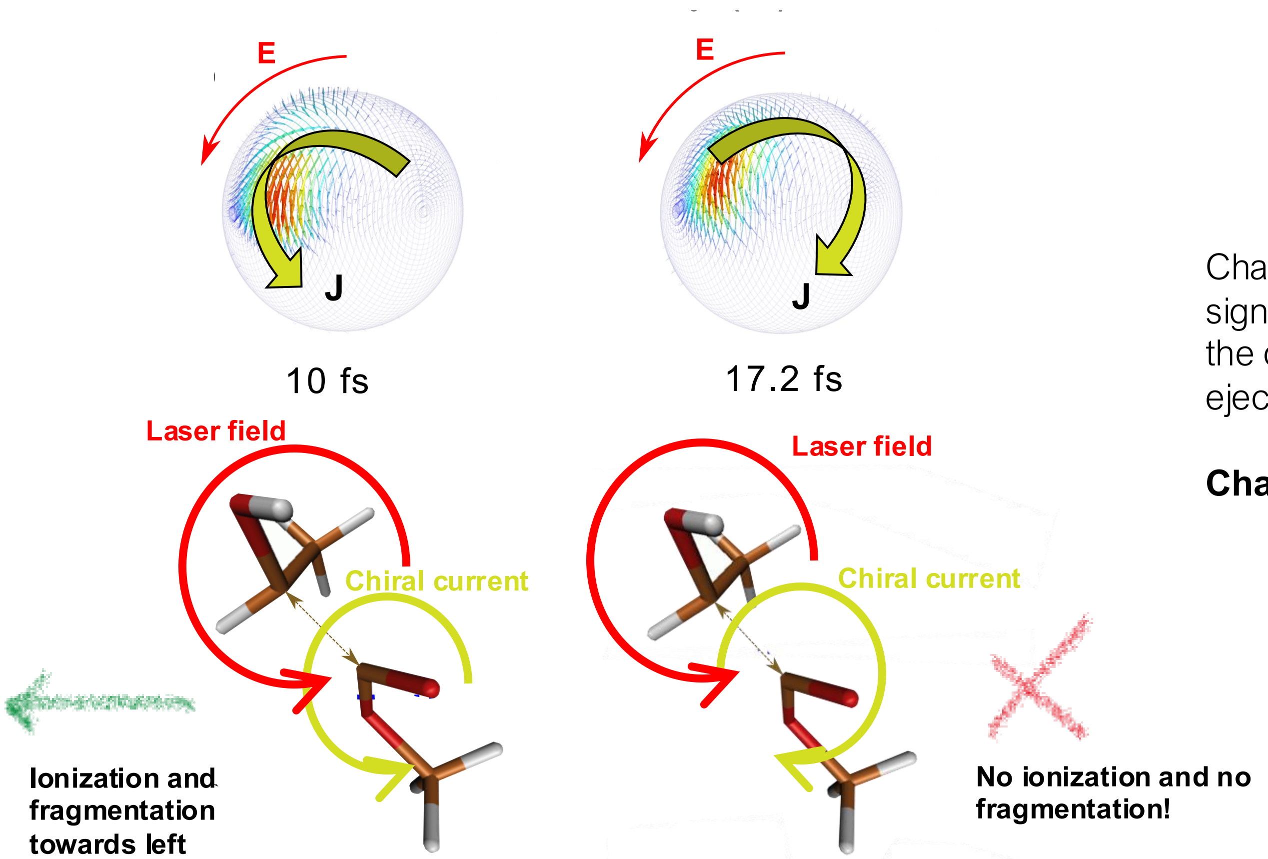

Charge migration dictates the sign of the chiral currents and the direction of the fragment ejection.

Charge-directed reactivity!

Collaboration with Olga Smirnova, MBI

Molecular orientation effects

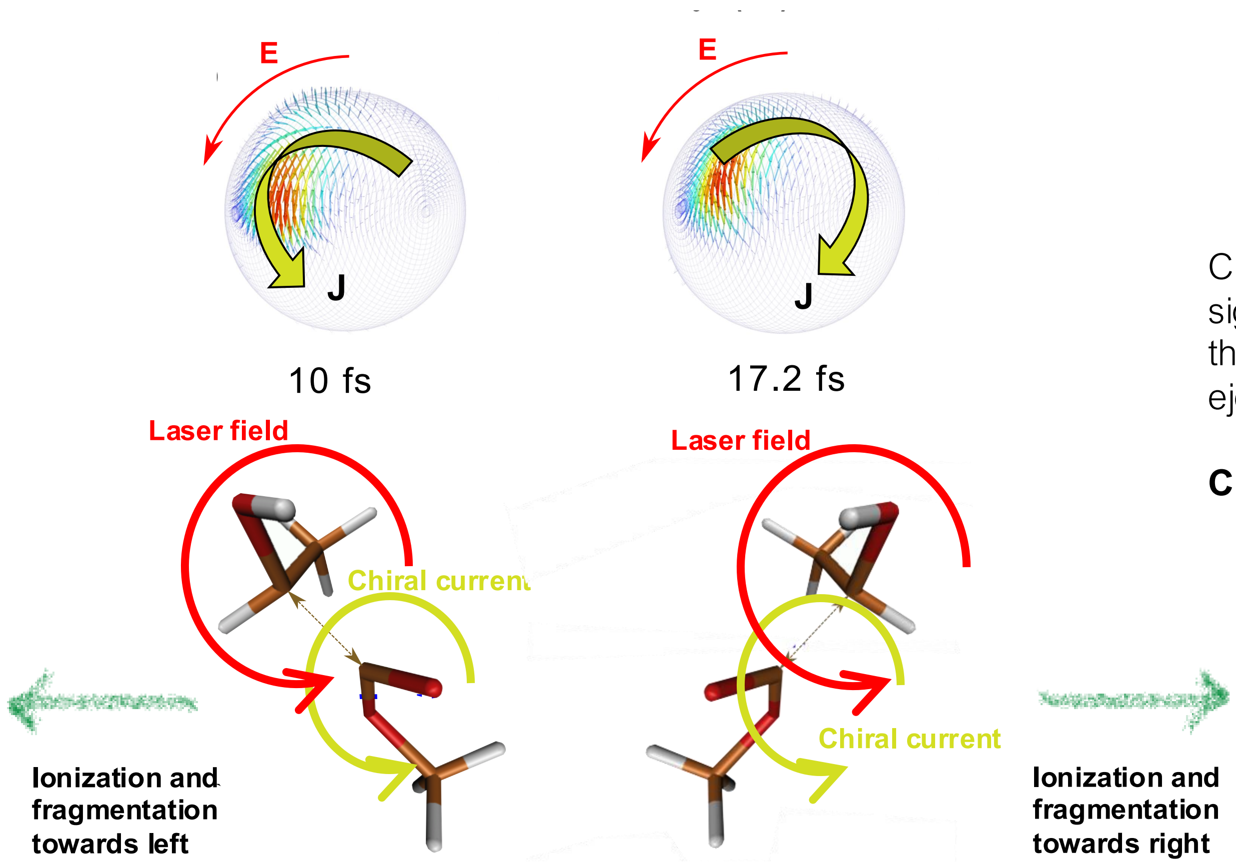

Charge migration dictates the sign of the chiral currents and the direction of the fragment ejection.

Charge-directed reactivity!

Collaboration with Olga Smirnova, MBI

Preliminary results in methyl lactate

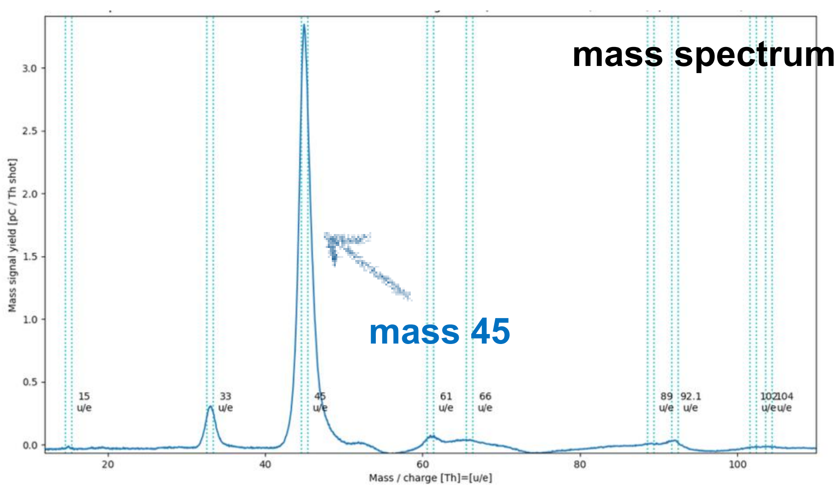

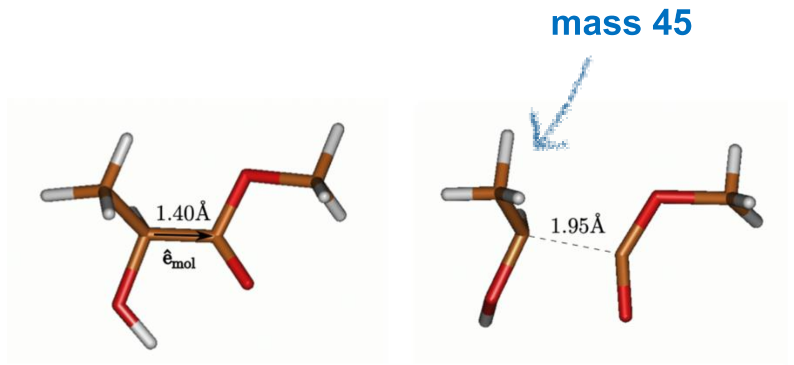

- Ion velocity map imaging (Ion VMI)
- Main contribution from fragment 45
- Breakage of C-C bond
- Covariance with ion ToF
- Measurement of RCP-LCP

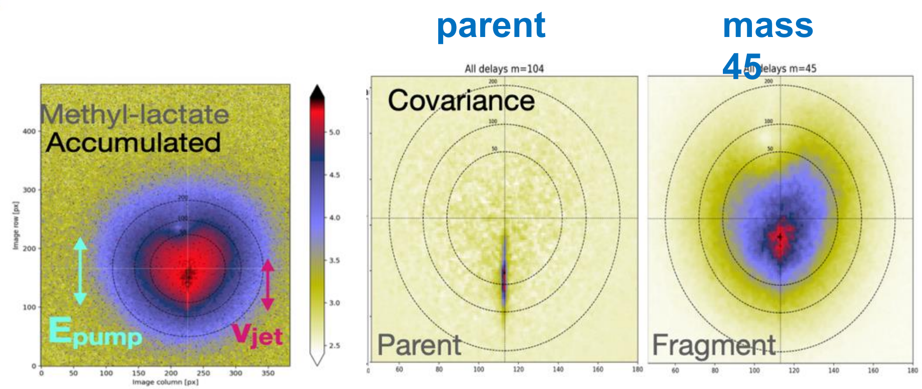

Time dependent asymmetry in the ions

FFT analysis of the momentum distribution (RCP-LCP)

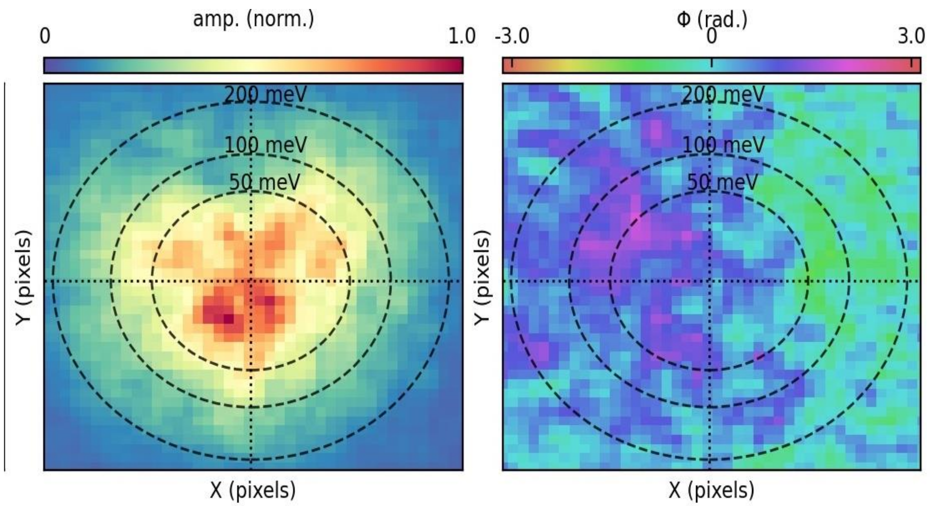

FFT amplitude at 200 meV

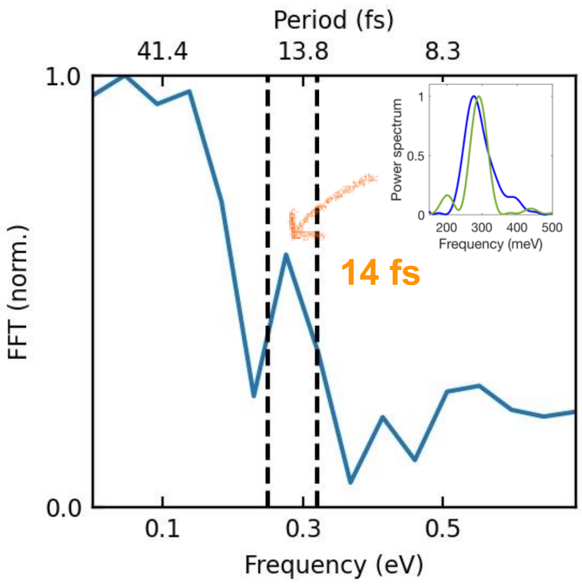

- Clear phase jump between the right and the left side of the FFT phase map
- FFT amplitude extracted at 200 meV shows the same periodicity of the PECD

Nanoplasmonics: photoemission delays and quantum effects

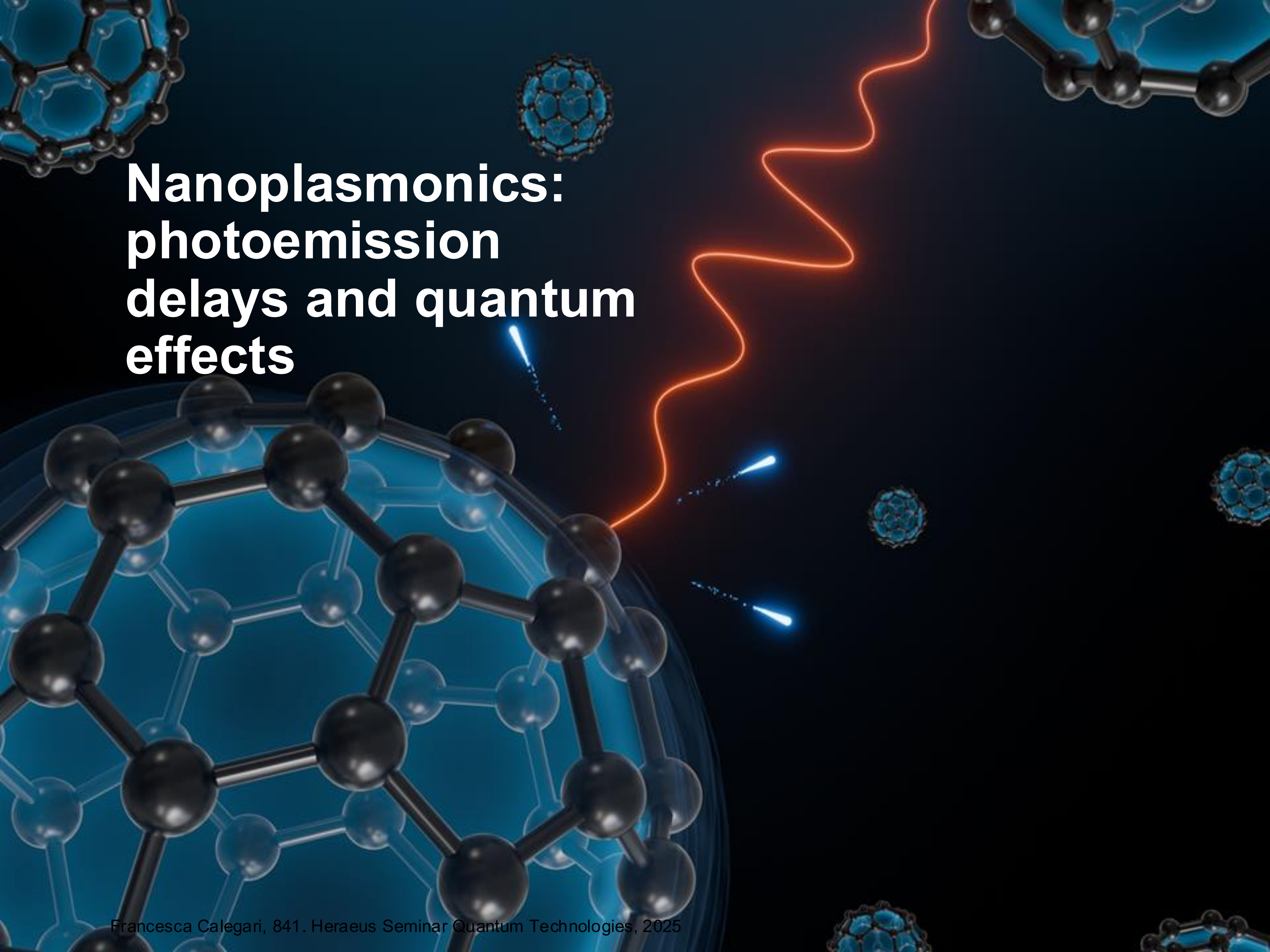

Attosecond chronoscopy of photoemission

We could see ionization as half-collision

Scattering phase: associated with an **advance** or **retardation** of the outgoing electron wavepacket caused by its interaction with the **scattering potential.**

Eisenbud–Wigner–Smith (EWS) delay: energy derivative of the partial-wave scattering phase

$$\tau_W = \frac{\partial \phi(\epsilon,\omega)}{\partial \epsilon}$$

Group delay accumulated by the electron wave-packet

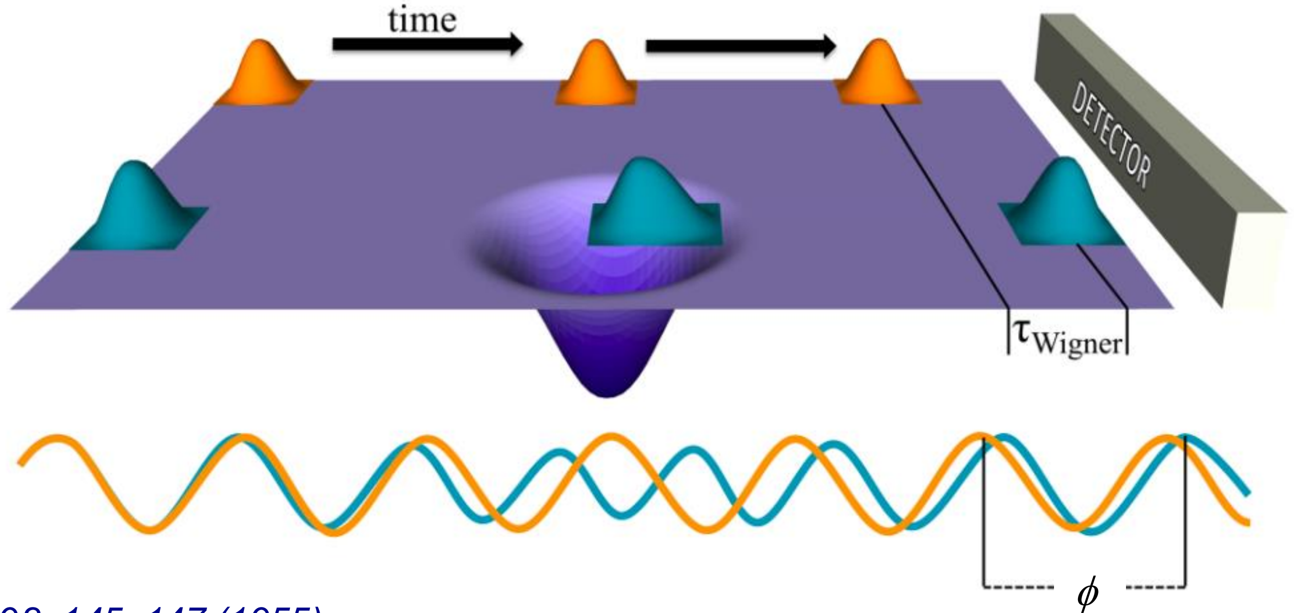

E. P. Wigner, Phys. Rev. 98, 145–147 (1955)
L. Eisenbud, Ph. D. thesis, Princeton University (1948)
F.T. Smith, Phys. Rev. 118, 349 (1960)
R. Pazourek et al, Rev. Mod. Phys. 87, 765–802 (2015)
L. Argenti, Phys. Rev A 95, 043426 (2017)

The RABBITT technique

RABBITT: reconstruction of attosecond beating by interference of two-photon transitions

Weak IR pulse + attosecond pulse train

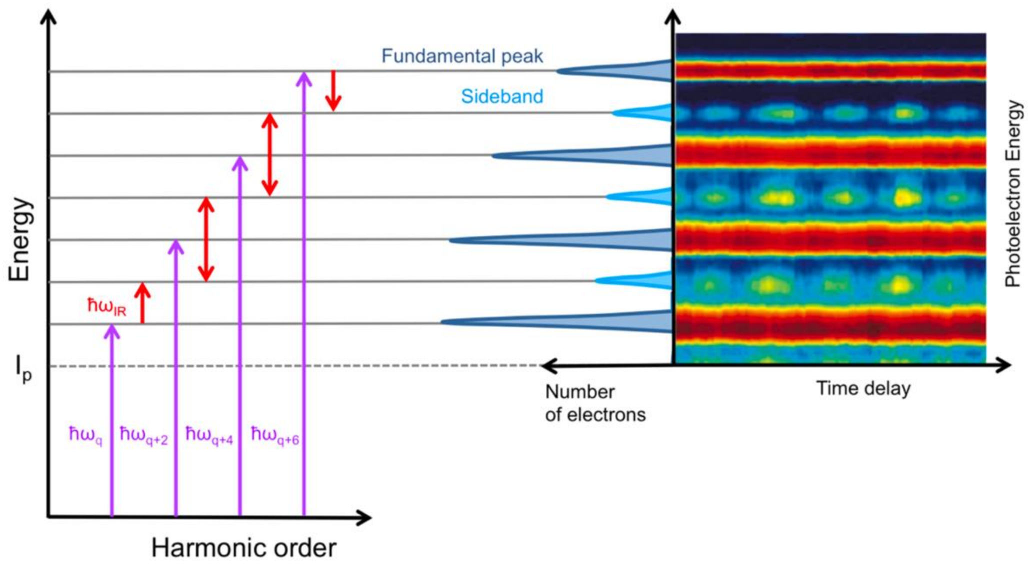

Ill. Niklas Elmehed © Nobel Prize Outreach

Pierre Agostini

Prize share: 1/3

P. M. Paul et al, Science 292,1689-1692 (2001)

Attochirp — Target scattering phase

Sidebands oscillations: $$\text{SB} \propto A\cos\left(2\omega_{IR}\tau - \Delta\varphi_{XUV} - \Delta\varphi_{\text{atomic}}\right)$$

Extracted delay: $$\tau_{\text{atomic}} = \hbar\frac{\partial\varphi_{\text{atomic}}}{\partial E} \cong \hbar\frac{\Delta\varphi_{\text{atomic}}}{\Delta E}$$

Photoemission delays extracted with RABBITT

Photoionization delay from Ne 2p and 2s

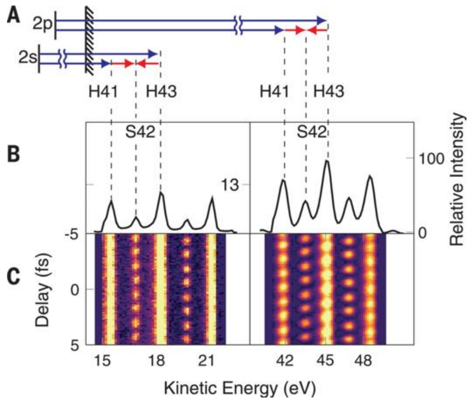

M. Isinger et al., Science 358,893-896 (2017)

Autoionization in He

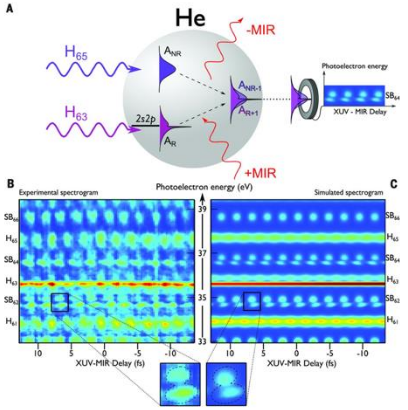

V. Gruson et al, Science 354,734-738 (2016)

Delay extracted from Ag surface reveals transport mechanisms

R. Locher et al, Optica 2, 405–410 (2015)

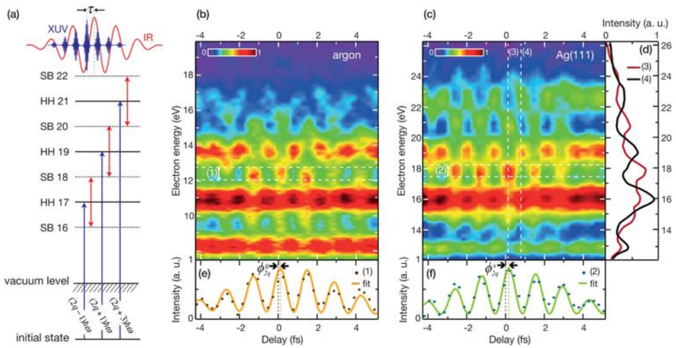

Photoemission delays extracted from liquid water

I. Jordan et al, Science, 369, 974-979 (2020)

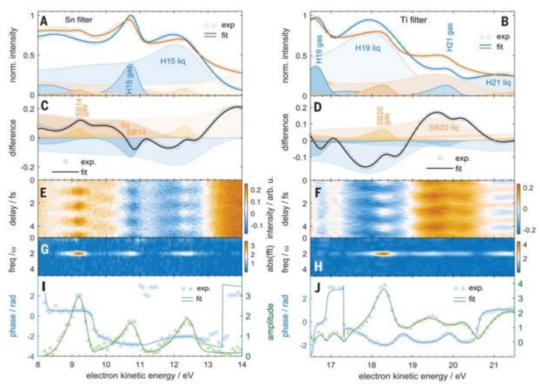

The streaking technique

Attosecond streak camera

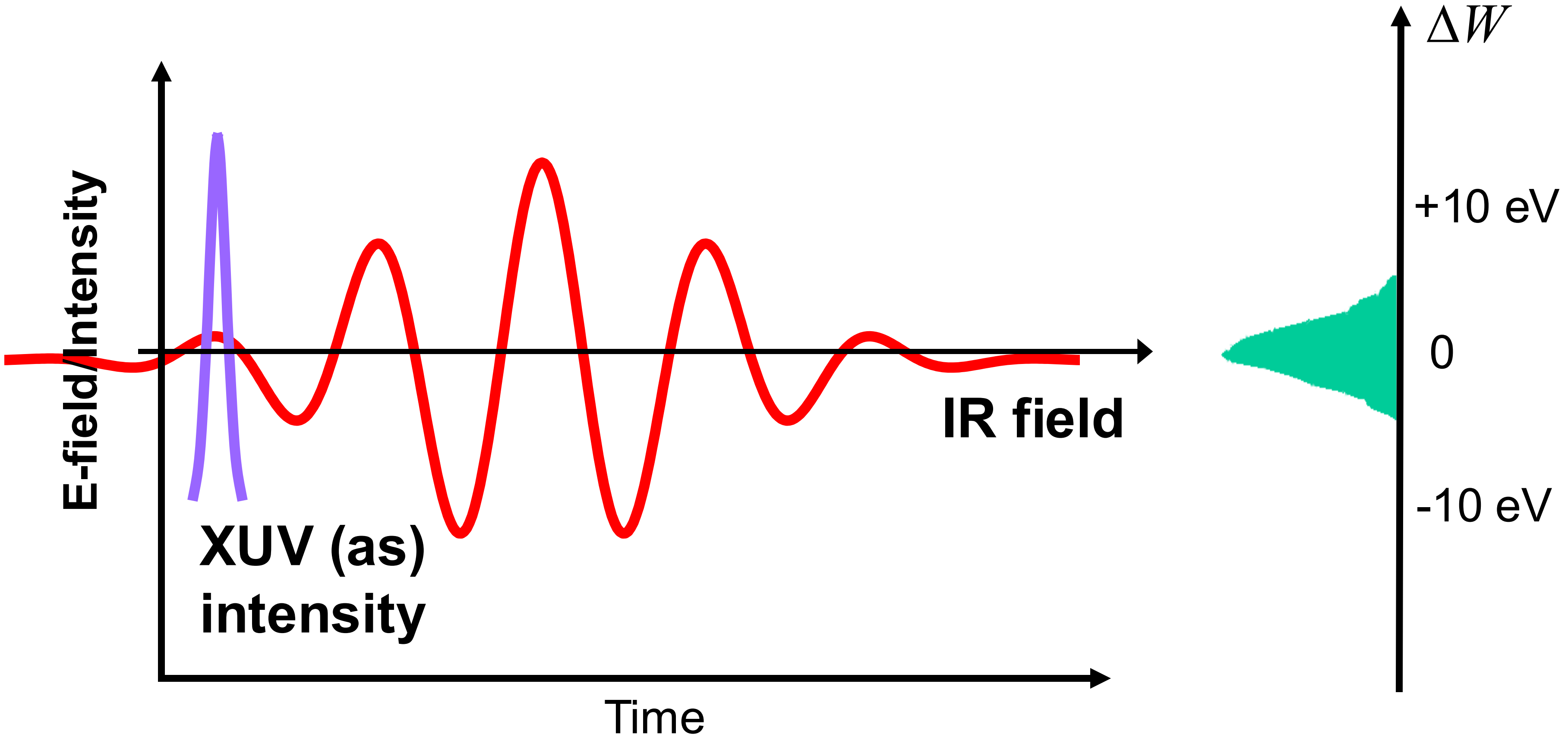

Hentschel, M. et al. Attosecond metrology. Nature 414, 509–513 (2001)

Extracting photoemission delays with attosecond streak camera

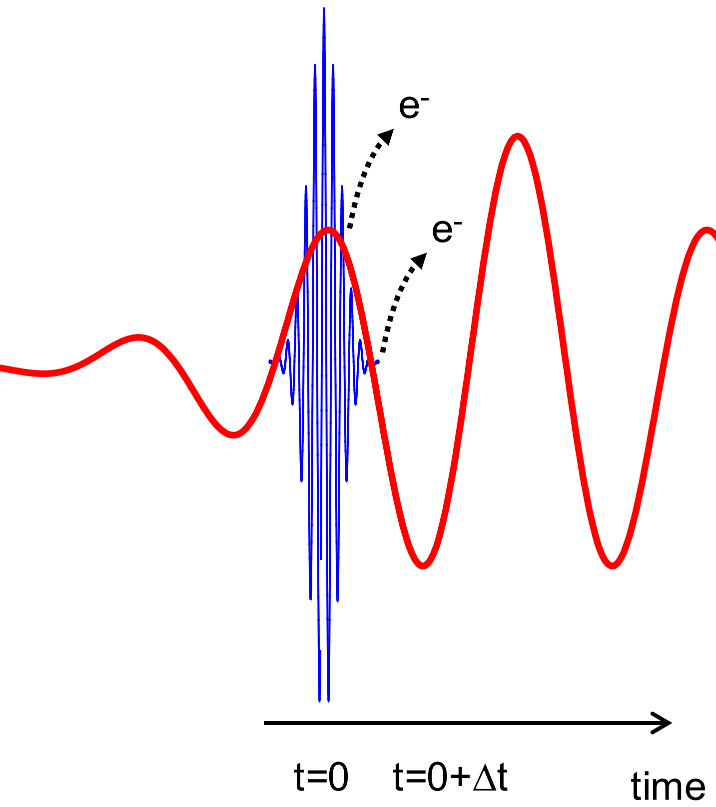

A delay in photoemission results in a delayed streaking trace

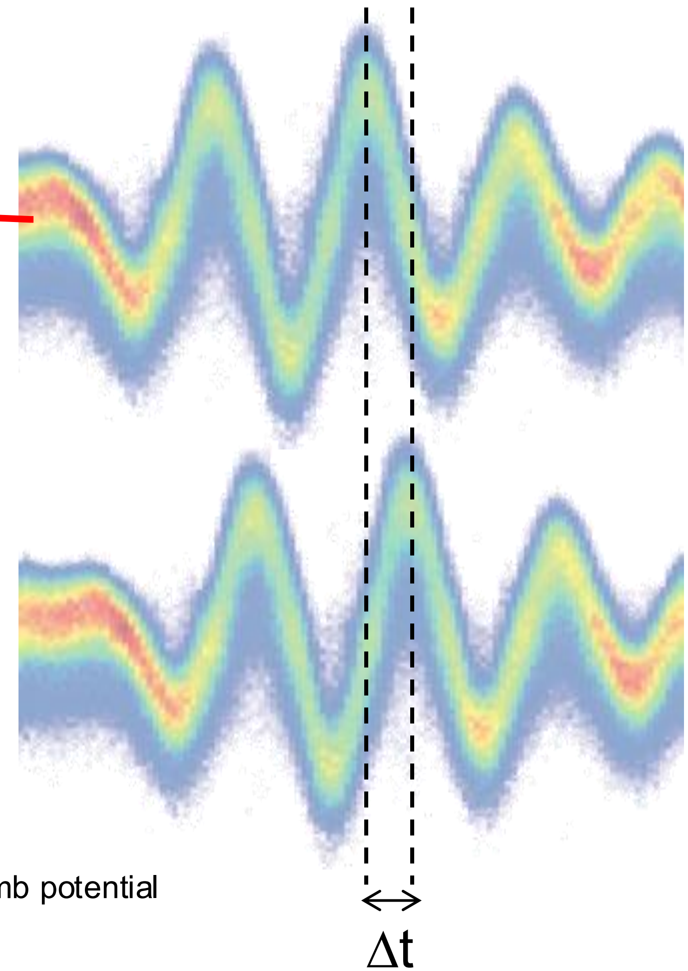

$$\Delta t = \tau_W + \tau_{CLC} + \tau_{attochirp}$$

τ_{CLC} : streaking field interacting with the asymptotic tail of the Coulomb potential
$\tau_{attochirp}$: residual chirp of the attosecond pulse

Photoemission delays with attosecond streak camera

Photoionization delay from Ne 2p and 2s

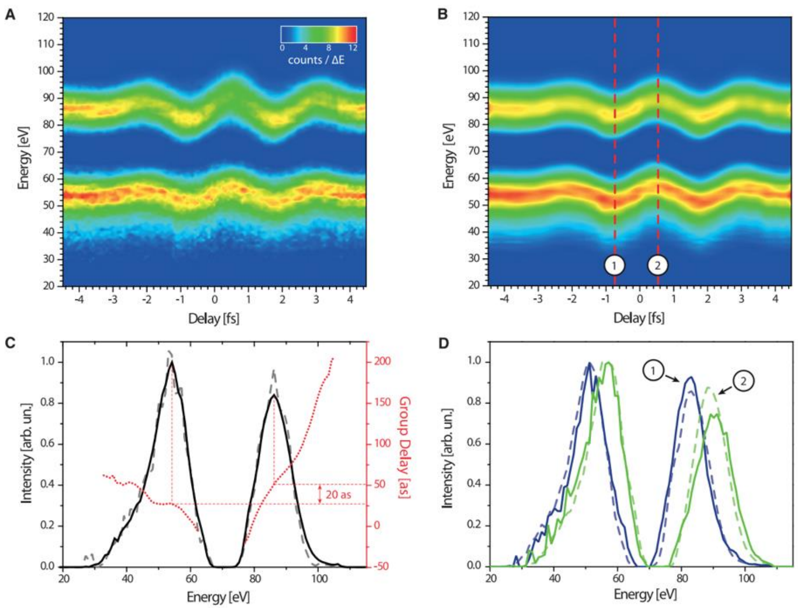

M. Schultze et al, Science 328, 1658-1662 (2010)

Photoemission delays from 4*f* states and conduction band of tungsten

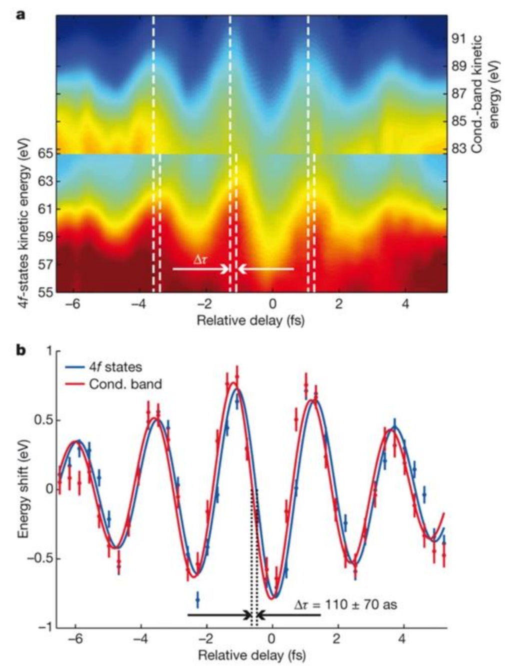

A. Cavalieri et al, Nature 449, 1029-1032 (2007)

Timescale of the surface plasmon evolution

- Plasmon resonances near metal surfaces concentrates the incident radiation far beyond the limits of the geometrical optics
- Classic interpretation: collective electron dynamics
- Fast dephasing routes
- Important applications: **solar energy harvesting, sensing, photocatalysis.**

N. Kholmicheva et al, Nanophotonics, vol. 8, no. 4, 2019, pp. 613-628.

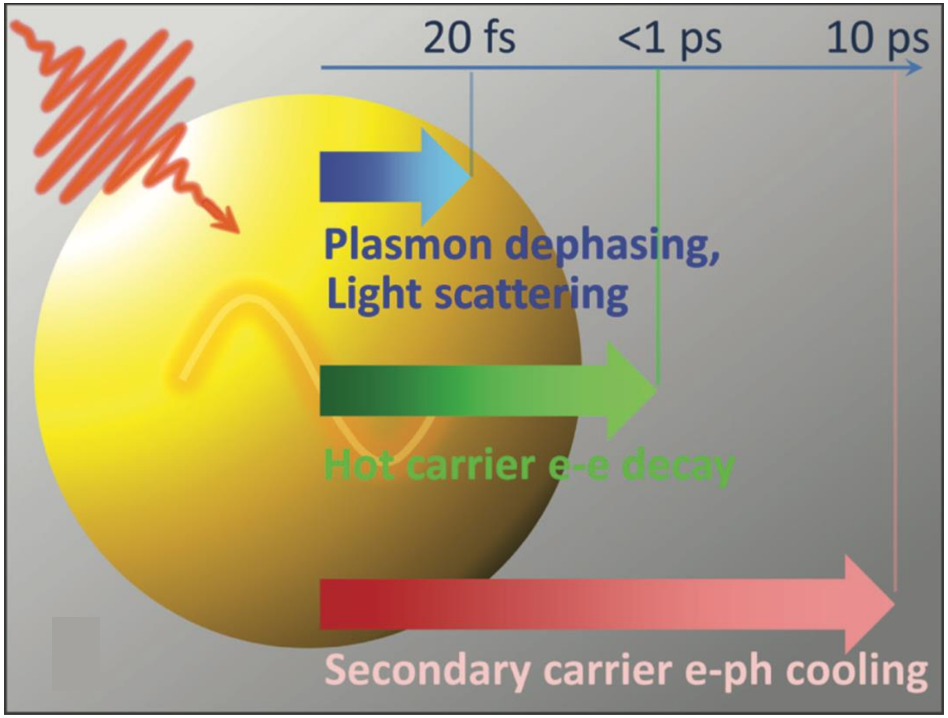

Plasmonics in the quantum limit

Sub-nm regime: quantum limit, ultrafast dephasing, role of electron correlations?

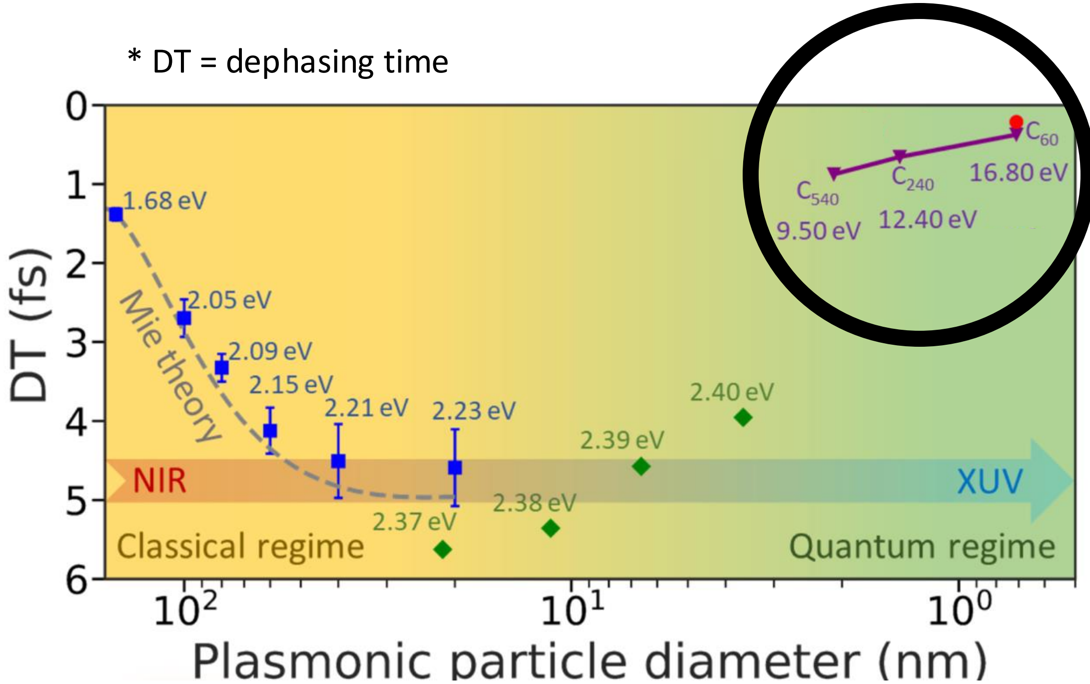

Fullerenes C_n

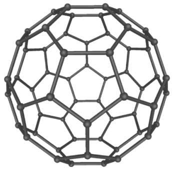

Sonnichsen, C., et al., New J Phys 4, 93 (2002)
Piella, J., et al., Chem Mater 28, 1066-1075 (2016)
Scholl, J. A., et al., Nature 483, 421-427 (2012)

The fullerene C_{60}

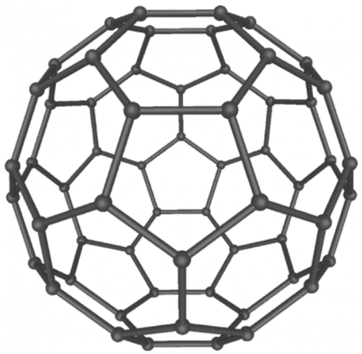

sub-nm diameter
240 valence electrons

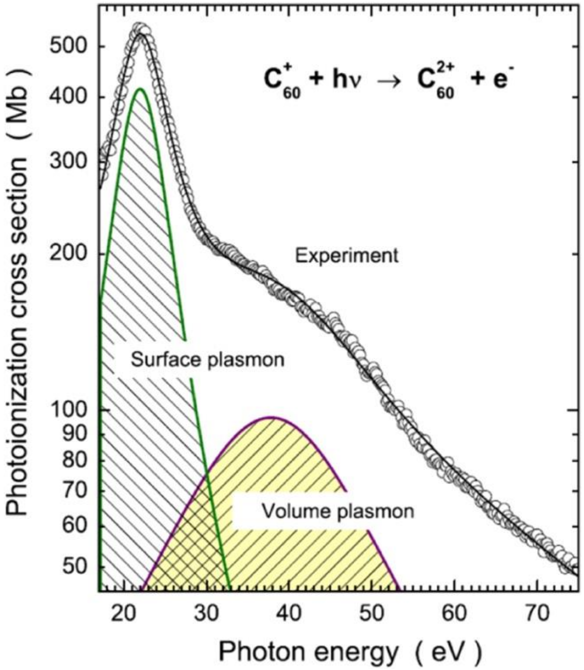

T. Barillot et al, Phys. Rev. A 91, 033413 (2015)
Hertel I, Phys. Rev. Lett., 68 784–7 (1992)
F. Lépine, J. Phys. B: Atomic, Mol. and Opt.Phys., 48, 12 (2015)

Ultrabroad (ultrafast) giant plasmonic resonance in the continuum (~20 eV, Ip ~7.6 eV).

Attosecond-resolution spectroscopy is required.

The experiment: attosecond streaking setup

Duration ~ 200 as

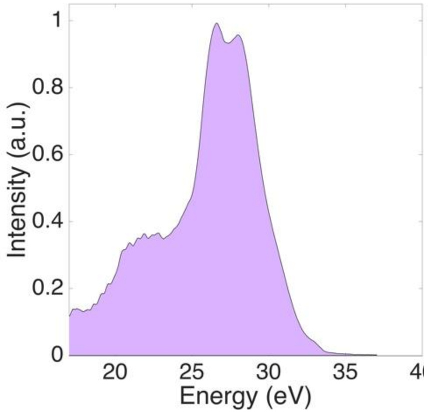

Duration ~ 4 fs

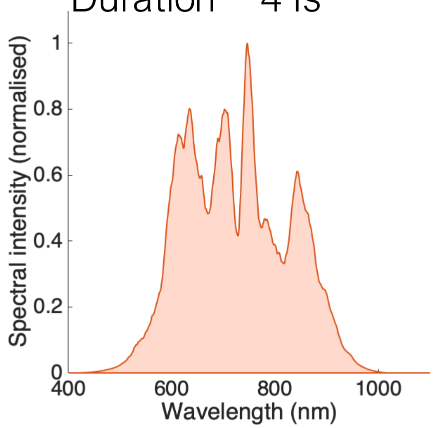

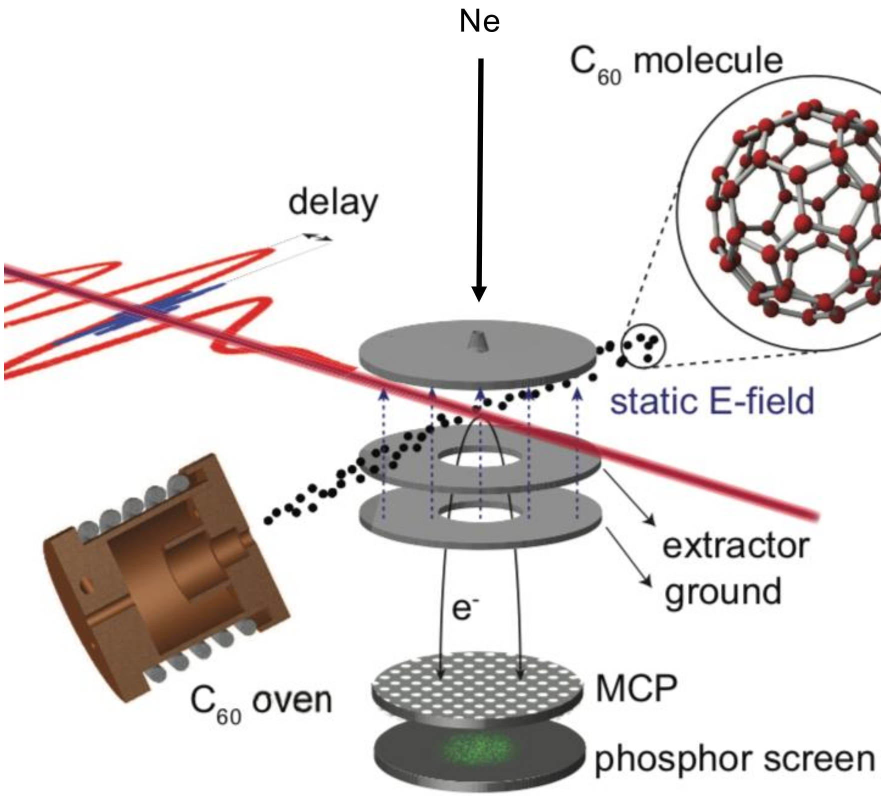

In collaboration with M. Kling, MPQ and Standford and M. Nisoli, Politecnico di Milano

Extraction of photoemission delays from C_{60}

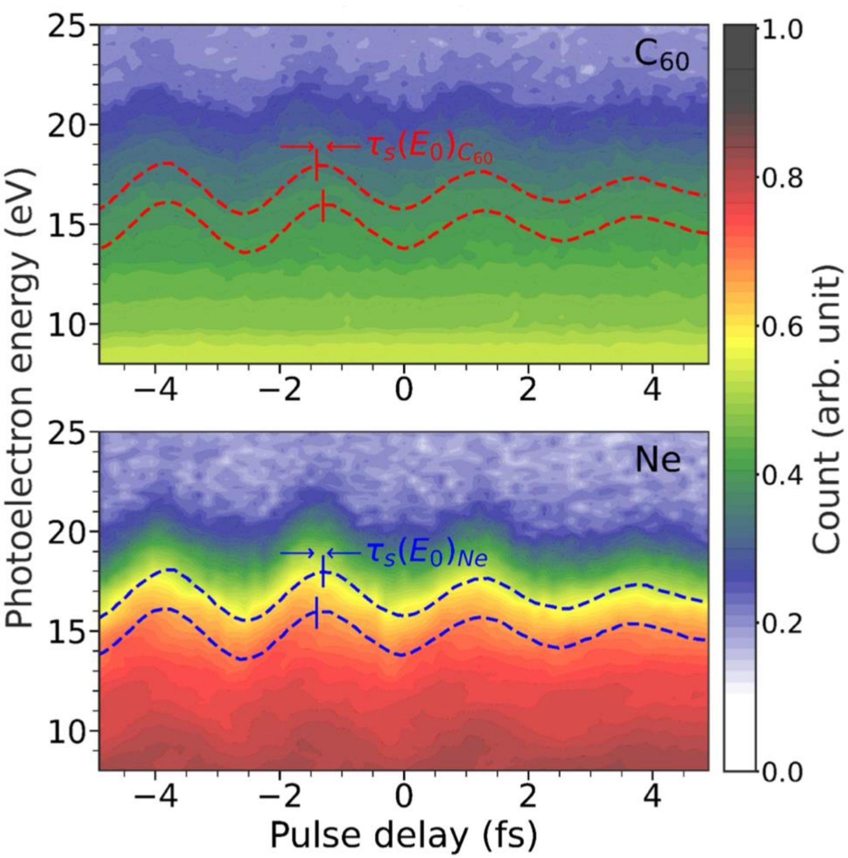

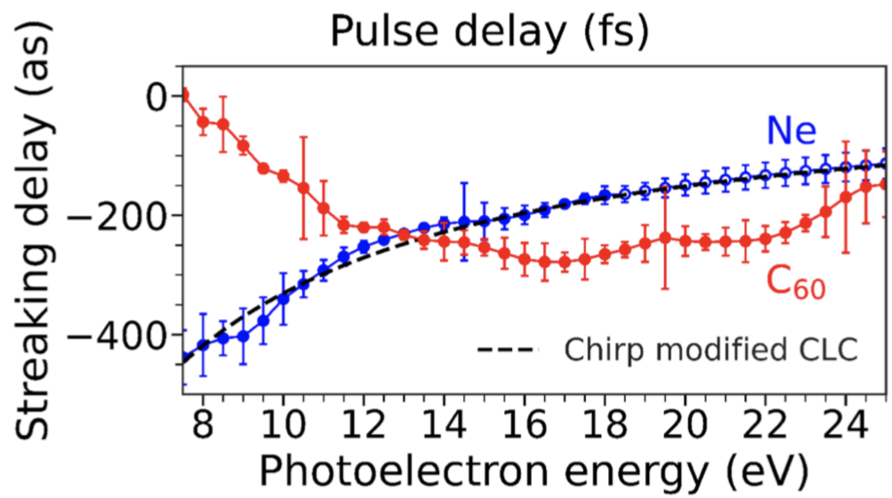

Streaking in neon is used to create a reference clock, characterize the attochirp and cancel out t_{CLC} :

$$\Delta t = (\tau_W + \cancel{\tau_{CLC}} + \cancel{\tau_{attochirp}} + \tau_{dipole})_{C60} - (\tau_W + \cancel{\tau_{CLC}} + \cancel{\tau_{attochirp}})_{Ne}$$

Role of quantum correlations

Theoretical modeling:

- Linear-response-TDDFT for the XUV-induced photoionization
- Classical trajectory Montecarlo simulations for the streaking where near-field effects are taken into account

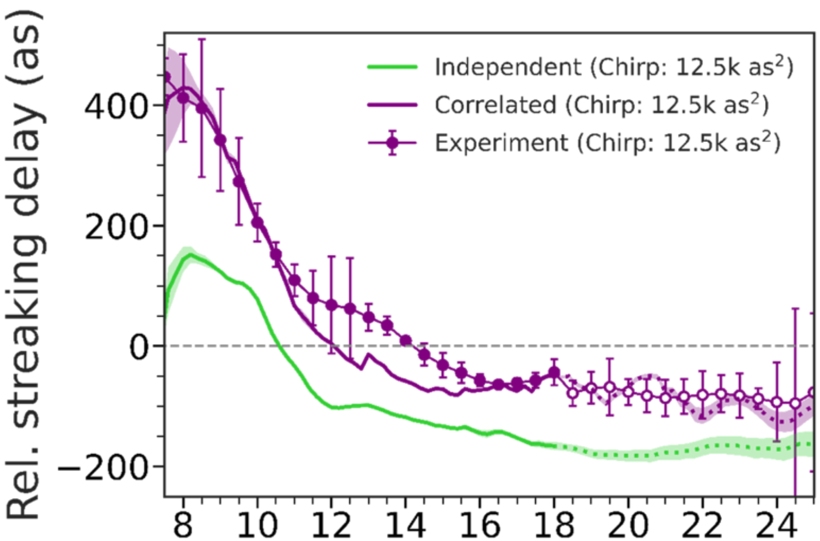

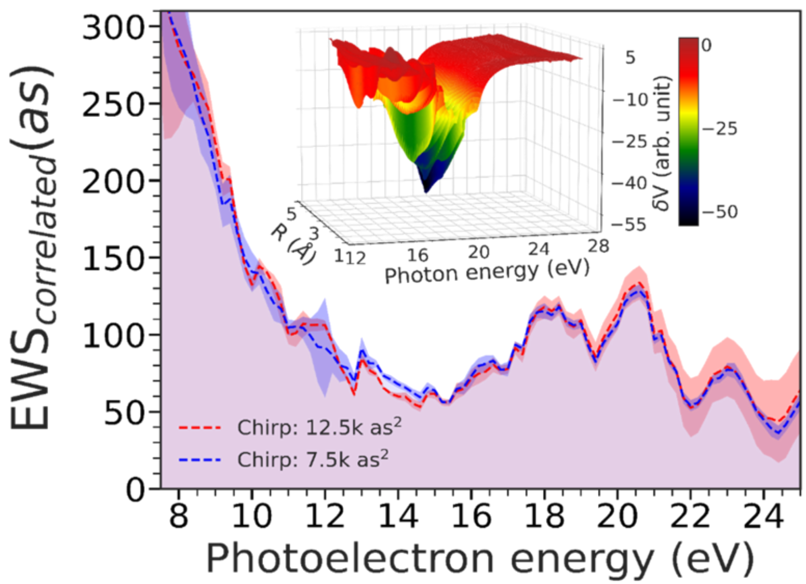

Photoionization is the fastest dephasing channel and it is **dominated by electron correlations.**

S. Biswas et al, Sci. Adv. 11, eads0494 (2025)

In collaboration with H. Himadri Chakraborty, M. Madjet, M.Magrakvelidze, Missouri University
U. De Giovannini, A. Rubio, MPSD, Hamburg

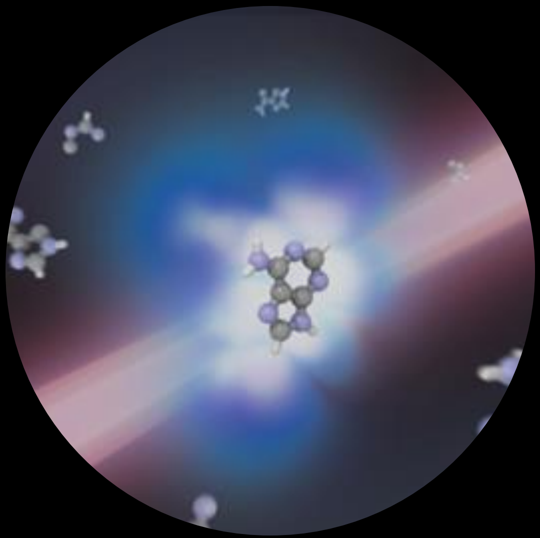

Observe electron migration in molecules

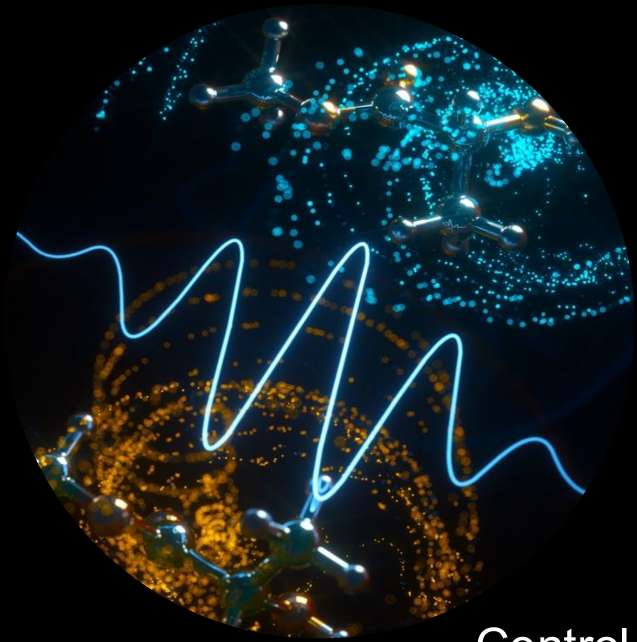

Control chiral optical response

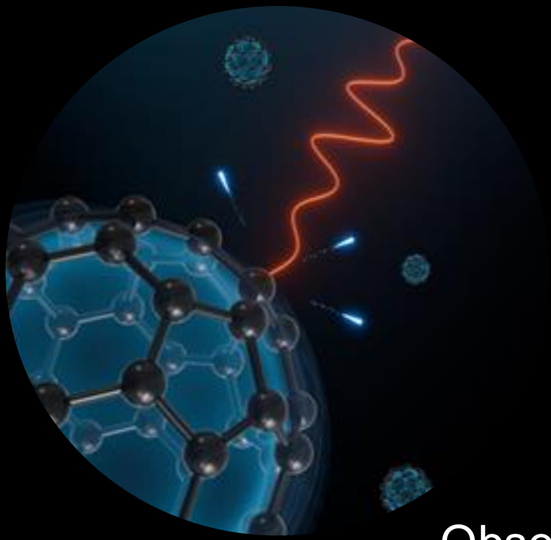

Observe quantum dynamics in nanosystems

Attosecond Science Group at DESY- CFEL

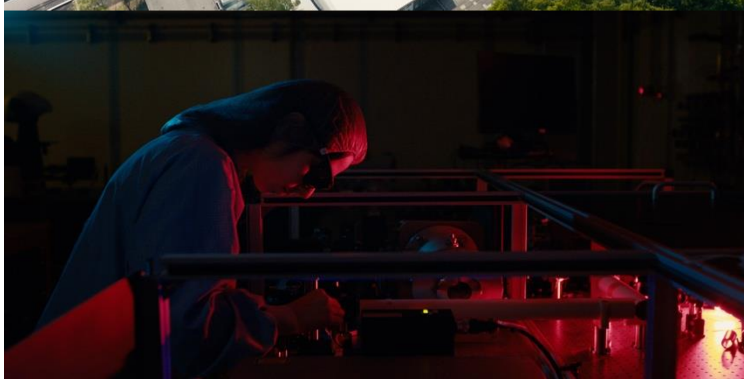

https://atto.cfel.de

- Attochemistry
- Ultrafast chirality
- Ultrafast nanoplasmonics
- Photoemission delays from complex targets
- Ultrafast dynamics in quantum materials

Thank you!

DESY-CFEL/ UHH

Agata Azzolin
Lorenzo Colaizzi (now Polimi)
Lorenzo Pratolli
Ana Ferreira de Oliveira e Silva
Erik Månsson
Sergey Ryabchuk
Ammar Bin Wahid
Sabine Rockenstein
Oliviero Cannelli
Vincent Wanie
Terry Mullins
Andrea Trabattoni (now DESY/Uni Hannover)

CELIA
Valerie Blanchet
Etienne Bloch
Yann Mairesse
Bernard Pons

MBI
Olga Smirnova

Imperial College
David Ayuso
Andres Ordonez

Université P. Sabatier
Nadia Ben Amor
Marie-Catherine Heitz

INRS
Francois Lègarè

MPSD
Angel Rubio
Umberto De Giovannini
Simone Latini

CNR-IFN
Rebeca Martinez-Vazquez
Roberto Osellame
Salvatore Stagira
Caterina Vozzi
Michele Devetta
Fabio Frassetto
Luca Poletto

LMU/MPQ/ Stanford
P. Rupp
Q. Liu
S. Biswas
M. F. Kling

Missouri State University
H. Chakraborty

University of Mary Washington
M. Magrakvelidze

European Research Council
Established by the European Commission

CLUSTER OF EXCELLENCE
CUI: ADVANCED IMAGING OF MATTER

SFB
SFB 925: Light induced dynamics and control of strongly correlated quantum systems

HELMHOLTZ RESEARCH FOR GRAND CHALLENGES

RöntgenÅngströmCluster

PIER

HELIOS
Helmholtz-Lund International Graduate School

AttoChem
Attosecond Chemistry